ANTIOXIDANTS & REDOX SIGNALING
Volume 24, Number 13, 2016

DOI: 10.1089/ars.2015.6586

Discoveries

FORUM REVIEW ARTICLE

HyPer Family Probes: State of the Art

Dmitry S. Bilan and Vsevolod V. Belousov

Abstract

Significance: Hydrogen peroxide (H_2O_2) is not only a key mediator of oxidative stress but also one of the most important cellular second messengers. This small short-lived molecule is involved in the regulation of a wide range of different biological processes, including regulation of cellular signaling pathways. Studying the role of H_2O_2 in living systems would be challenging without modern approaches. A genetically encoded fluorescent biosensor, HyPer, is one of the most effective tools for this purpose. ***Recent Advances:*** HyPer has been used by many investigators of redox signaling in various models of different scales: from cytoplasmic subcompartments and single cells to tissues of whole organisms. In many studies, the results obtained using HyPer have enabled a better understanding of the roles of H_2O_2 in these biological processes. However, much remains to be learned. ***Critical Issues:*** In this review, we focus on the uses of HyPer. We provide a general description of HyPer and its improved versions. Separate chapters are devoted to the results obtained by various groups who have used this biosensor for their experiments in living cells and organisms. ***Future Directions:*** HyPer is an effective tool for H_2O_2 imaging in living systems as indicated by the increasing numbers of publications each year since its development. However, this biosensor requires further improvements. In particular, much brighter and more pH-stable versions of HyPer are necessary for imaging in mammalian tissues. *Antioxid. Redox Signal.* 24, 731–751.

Introduction

In aerobic organisms, oxygen plays a central role in the maintenance and regulation of vital redox reactions. Specifically, oxygen is the final acceptor of electrons in the respiratory electron transport chains involved in cellular energy production. However, the role of oxygen is not limited to respiration. Regulatory, or signaling, functions of oxygen are carried out by reactive oxygen species (ROS).

ROS are produced in many biochemical processes both spontaneously and through regulated mechanisms. Superoxide anion radical $O_2^{\bullet-}$ is a precursor of all other types of ROS. $O_2^{\bullet-}$ is formed by univalent reduction of molecular oxygen O_2. Cellular electron transport chains are one of the sources of $O_2^{\bullet-}$ in the cells. In eukaryotes, it is generated by the mitochondrial respiratory chain at the levels of complex I (NADH:ubiquinone oxidoreductase) and complex III (ubiquinol:cytochrome c oxidoreductase) (24, 173, 200, 211). From 0.15% to 2% of the total, electron flow through the mitochondrial respiratory chain supports ROS generation (31, 200).

NOX (nicotinamide adenine dinucleotide phosphate oxidase) family proteins are the main source of cellular $O_2^{\bullet-}$. These membrane enzyme complexes transfer electrons across biological membranes using NADPH as an electron donor. Oxygen serves as an electron acceptor, which leads to the formation of substantial amounts of $O_2^{\bullet-}$ (6, 10). Xanthine oxidase that is involved in oxidation of purines and nitric oxide synthases (NOSs) catalyzing the production of nitric oxide are the other examples of enzymes that may contribute to the cellular production of $O_2^{\bullet-}$ (23, 137). The majority of cellular $O_2^{\bullet-}$ is converted into hydrogen peroxide (H_2O_2) by highly specialized enzyme, superoxide dismutase (SOD), almost immediately (136). Thus, SOD neutralizes the radical and prevents its devastating effects. However, H_2O_2 can be toxic for cells as well. Regulation of cellular H_2O_2 is controlled by several enzymatic systems such as catalases (31, 33), peroxiredoxins (Prxs) (96, 219), and glutathione peroxidases (GPxs) (67).

For many decades, ROS were believed only to be damaging oxidative stress molecules because of their ability to

Shemyakin-Ovchinnikov Institute of Bioorganic Chemistry, Moscow, Russia.

cause oxidative damage to different cellular molecules and structures (53, 198), and ROS are clearly involved in the induction and progression of many pathological states as well as in the aging process. However, ROS are also produced, at lower levels, in normal physiological processes, in which they play important roles in cellular functions (53, 178). The concentrations and lifetimes of ROS in cells are strictly controlled by specialized enzymatic systems.

After discovery of NOX2 in phagocytic cells and the establishment of its role in the pathogen elimination (7, 44, 152, 155, 172), other members of this protein family were found to exist in a large variety of nonphagocytic cell types (10). The variety of ubiquitous NOX homologues that generate $O_2^{\bullet-}$ in cells of different tissues is one more proof that ROS play an active role in the regulation of cellular processes. Particular attention among ROS is given to H_2O_2, which is now regarded as a second messenger.

The signaling role of H_2O_2 stems from its ability to selectively modify the thiol groups of certain proteins, thereby regulating their functions (34, 210). Modifications of amino acids can significantly affect the conformation of proteins, changing their functionality or interaction with partners. Oxidation by H_2O_2 is one of the cysteine modifications allowing protein function modulation either *via* catalytic Cys inactivation or conformational rearrangements. Accessibility and pK_a values of cysteine residues in the protein structure are the main factors limiting H_2O_2 interaction with proteins.

Accessibility of cysteines for interaction with H_2O_2 depends on structural characteristics of a particular protein. Usually, cysteines that interact with H_2O_2 and participate in cell signaling are exposed and available for interaction. The location of two redox-active cysteines of peroxiredoxins is one of the bright examples among proteins interacting with H_2O_2 (218). Thiol groups of cysteines interacting with H_2O_2 usually have a pK_a value lower than most of thiol groups not involved in such reactions due to the local environment of the cysteine residues (217). Reaction of thiol groups with H_2O_2 leads to formation of a sulfenic acid, which can be oxidized to the more stable sulfinic acid or reduced again after disulfide formation (166). Sulfenic acid anions react with thiol groups of low-molecular-weight compounds as glutathione or with protein thiols forming intra/intermolecular disulfides (39). In a cell, these oxidative modifications are reversible due to the thiol/disulfide exchange catalyzed by glutaredoxins (Grxs) (63, 122) and thioredoxins (Trxs) (4, 40, 97).

Many examples of the involvement of H_2O_2 in the regulation of cell signaling pathways are available. The first discovered and best known example is an interaction of H_2O_2 with the active center of protein tyrosine phosphatases (PTPs), which leads to the inhibition of the phosphatase activity (48, 119). By contrast, H_2O_2 activates certain protein tyrosine kinases (PTKs), including Src family kinases (76). It is known that elevation of H_2O_2 leads to activation of mitogen-activated protein kinases (MAPKs), including the extracellular signal-regulated kinases (ERKs), jun N-terminal kinase (JNK), and p38 (170), which participate in many cellular signaling cascades (26).

Additionally, some cellular ion channels are regulated by H_2O_2. Examples of redox-regulated channels include, but are not limited to, Ca^{2+}-activated voltage-dependent K^+ channels ($K_{V,Ca}$) (195, 203) and ryanodine receptor (RyR) channels. Insulin-induced H_2O_2 generation causes RyR1 S-glutathionylation that leads to Ca^{2+} release (41). It has also been shown that the function of several transcription factors in cells also depends on H_2O_2 (125). The OxyR protein of *Escherichia coli* is the most studied example among such regulators (37).

It is not surprising that H_2O_2 has attracted enormous interest from investigators in the redox biology field. Several synthetic indicators for H_2O_2 detection in cells such as 2,7-dichlorodihydrofluorescein (DCFH), dihydrorhodamine 123 (DHR), Peroxy Green 1 (PG1), Peroxy Crimson 1 (PC1), and others are currently used (45, 68, 79, 143, 177). However, application of some of these probes is possible only *in vitro*. Typically, dyes that are able to penetrate into the cells are not specific for the individual forms of ROS and their reactions are irreversible. In addition, the signals of these indicators can be affected by artifacts associated with nonspecific reactions (68, 79).

Many of the problems of spectroscopic H_2O_2 detection methods were overcome by the genetically encoded fluorescent biosensors. Two types of genetically encoded sensors for H_2O_2 currently exist: HyPer, which was developed in 2006 (11), followed by other HyPer family members, and roGFP2-Orp1 (86). The principle of roGFP2-Orp1 and its applications have been extensively discussed in other reviews (139, 188). In a short period of time, HyPer has proven to be a powerful tool for the investigation of the dynamics and roles of H_2O_2 in various biological models. This biosensor allows real-time imaging of H_2O_2 in living systems of various complexities. Furthermore, its reaction is reversible and highly specific with regard to other types of ROS and various oxidants (11). This review will focus on how and where the sensor can be used.

Features of HyPer and Its Modifications

HyPer

The genetically encoded biosensor HyPer (from Hydrogen Peroxide) enables real-time imaging of H_2O_2 within cells and even individual compartments of the cell. The biosensor consists of the H_2O_2-sensitive regulatory domain of the *E. coli* transcription factor, OxyR, with the circularly permuted yellow fluorescent protein (cpYFP) integrated into the sequence of OxyR (11).

The transcription factor, OxyR, activates the expression of a number of antioxidant genes in bacteria in response to increasing concentrations of H_2O_2, thus protecting the cells from oxidative stress. The C-terminal domain of OxyR functions as a sensor for H_2O_2 by selectively and reversibly reacting with H_2O_2 (118, 227). Oxidation of OxyR by H_2O_2 causes the formation of a disulfide bond between cysteine residues, Cys-199 and Cys-208, in the structure of the regulatory domain, which leads to conformational changes in the DNA-binding domain of the protein. The selectivity of OxyR toward H_2O_2 is determined by the low pKa of Cys-199 and its hydrophobic environment (5, 37, 227). The disulfide bond in the oxidized OxyR can be reduced enzymatically by glutaredoxins and most likely by some other enzymes (227).

In the HyPer molecule, the OxyR domain performs the same function. cpYFP is integrated into the sequence of the C-terminal regulatory OxyR domain in a position between amino acids, 205 and 206, *via* short peptide linkers. This region of OxyR is characterized by the most significant changes in the structure upon oxidation–reduction. The OxyR domain of HyPer is

specifically oxidized by H_2O_2 and undergoes conformational changes that are transmitted to the fluorescent protein (FP; a schematic representation is shown in Fig. 1A). The spectral characteristics of HyPer change as a result of these intramolecular reorganizations. The fluorescence excitation spectrum of HyPer has two maxima at 420 and 500 nm and a single emission peak with a maximum at 516 nm. Upon oxidation of HyPer in the presence of H_2O_2, the intensity of the 420 nm excitation peak decreases proportionally to the increase in the 500 nm peak (Fig. 1B). Therefore, HyPer is a ratiometric sensor. In living systems, for example, in cells as shown in Figure 1C, the HyPer signal should be defined as the ratio of fluorescence intensities separately excited at 500 and 420 nm (F_{500}/F_{420}). Increasing of H_2O_2 concentration results in oxidation of the biosensor, and the F_{500}/F_{420} signal increases (Fig. 1C, D) (11).

In vitro, minimal response of fully reduced HyPer protein at a concentration of 25 n*M* can be observed after addition of 25 n*M* of H_2O_2 (fold change in F_{500}/F_{420} ratio is 1.5 ± 0.12). The addition of 250 n*M* of H_2O_2 to the probe leads to full oxidation of the biosensor (11). The same sensitivity was confirmed for HyPer in the cytoplasm of mammalian cells. Minimal concentration of externally added H_2O_2 that induces minimal detectable changes in HyPer fluorescence is 5 μM (11). According to the experimental data, the gradient of H_2O_2 across the plasma membrane can reach 650-fold (98). Therefore the sensitivity and specificity of HyPer to H_2O_2 are similar to these parameters in the wild-type OxyR, and similar to the wild-type OxyR, oxidized HyPer is reduced by cellular thiol-reducing systems (11).

HyPer is currently being successfully used in many laboratories to study the roles of H_2O_2 in living systems. However, in some biological models, the average cytoplasmic concentration of signaling H_2O_2 changes very little relative to the basal level. Despite its 3-fold ratio change upon reaction with saturating amounts of H_2O_2, the dynamic range of HyPer is not high enough to visualize these small changes in H_2O_2 concentration. Therefore, it was very desirable to improve the dynamic range (R/R_0) of HyPer.

HyPer-2 and HyPer-3—improved versions of HyPer

HyPer-2 was the first improved version of the biosensor (131). HyPer-2 demonstrates an expanded dynamic range compared with the parental HyPer. The F_{500}/F_{420} ratio of HyPer-2 changes up to 6–7-fold upon saturation of the probe, which is twice as high as that of HyPer. This means that at lower oxidant concentrations, the HyPer-2 response is twice as easy to visualize. The advantage of using HyPer-2 to monitor low concentrations of endogenous H_2O_2 was demonstrated in NIH 3T3 fibroblasts stimulated with the platelet-derived growth factor (PDGF). HyPer-2 demonstrated higher amplitude of response than HyPer in the same cells.

HyPer-2 differs from HyPer only by one point mutation: Ala406Val (131). This mutation is located in the OxyR domain of HyPer. The same mutation was previously described in the wild-type OxyR. It resides in the interface responsible for the oligomerization of the protein (37). Unlike the original HyPer molecule, which is monomeric, HyPer-2 forms a strong dimer. HyPer-2 also has lower rates of reaction with H_2O_2 and subsequent reduction in the cells than those of HyPer (16, 131) (Fig. 2A, B). These deficiencies could potentially affect the temporal resolution of the H_2O_2 detection.

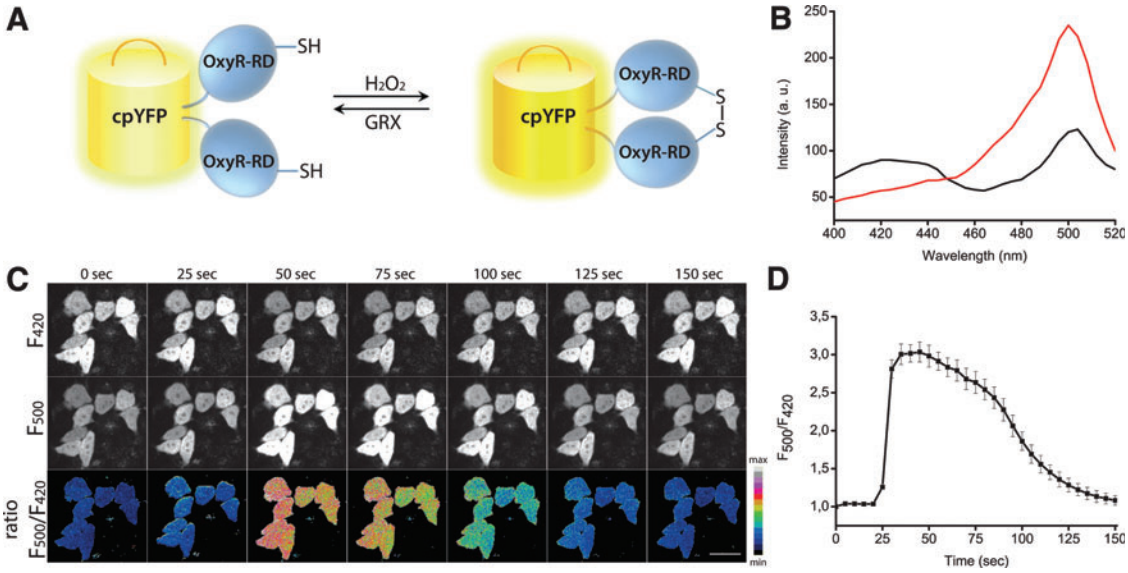

FIG. 1. Genetically encoded fluorescent biosensor HyPer for H_2O_2 measuring. (A) The scheme of HyPer structure and its oxidation and reduction reactions. **(B)** Excitation spectrum of reduced (*black line*) and full oxidized (*red line*) protein HyPer extracted from *Escherichia coli*. Two excitation peaks of HyPer with maxima at 420 and 500 nm ratiometrically change upon oxidation. Emission was measured at 530 nm. **(C)** Images of HyPer-expressing HeLa Kyoto cells at indicated time points before and after addition of 75 μM of H_2O_2 (H_2O_2 was added after 20 s). In two *upper rows*, fluorescence of HyPer was excited in two channels at 420 and 500 nm (F_{420} and F_{500}), respectively. *Lowest row* represents the F_{500}/F_{420} excitation ratio. Scale bar, 40 μm. *Lookup table* indicates the F_{500}/F_{420} ratio. **(D)** HyPer response (F_{500}/F_{420} ratio) to added H_2O_2 in mammalian cells shown in **(C)**. Error bars indicate standard error of mean. To see this illustration in color, the reader is referred to the web version of this article at www.liebertpub.com/ars

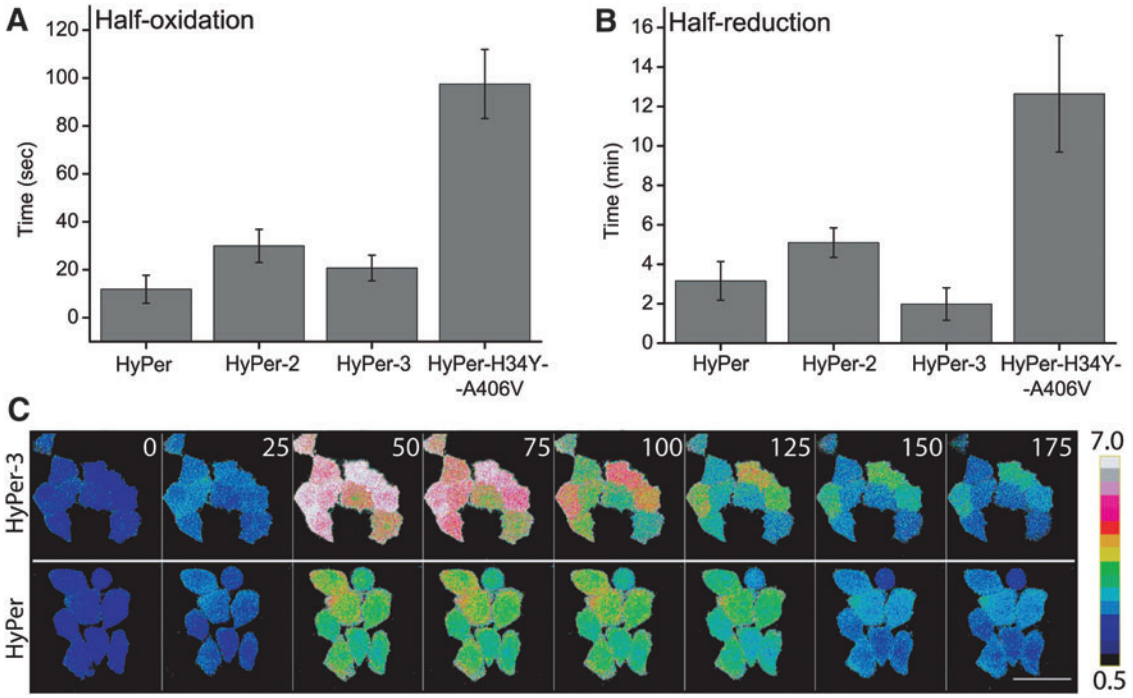

FIG. 2. HyPer, HyPer-2, and HyPer-3 response to H_2O_2 [Reprinted with permission from Bilan *et al.*, (16)]. **(A)** Half-oxidation times of HyPer, HyPer-2, HyPer-3, and HyPer-H34Y-A406V upon the addition of H_2O_2. Zero time corresponds to the moment of H_2O_2 addition. Error bars indicate standard deviation. **(B)** Half-reduction times of HyPer, HyPer-2, HyPer-3, and HyPer-H34Y-A406V upon the addition of H_2O_2. Zero time corresponds to the maximum of F500/F420 ratio after H_2O_2 addition. Error bars indicate standard deviation. Data in panels **(B)** and **(C)** are results of 7 experiments for HyPer, 10 for HyPer-2, 10 for HyPer-3, and 4 for HyPer-H34Y-A406V; >10 cells in each experiment. **(C)** Images of F_{500}/F_{420} ratio in HeLa cells transiently transfected with HyPer-3 (*upper row*) or HyPer (*lower row*) exposed to 150 μM of H_2O_2. *Numbers* indicate timing in seconds. Scale bar, 40 μm. *Lookup table* indicates the F_{500}/F_{420} ratio. To see this illustration in color, the reader is referred to the web version of this article at www.liebertpub.com/ars

A more rapidly responsive version was subsequently developed and was named HyPer-3 (16). HyPer-3 contains the mutation, His34Tyr, located in the same interface of OxyR as the mutation, Ala406Val, of HyPer-2. The dynamic range of HyPer-3 is comparable with that of HyPer-2 (6–7-fold). However, the reaction rates of oxidation and reduction of HyPer-3 are higher than those of HyPer-2 (Fig. 2). The oligomeric states of HyPer-2 and HyPer-3 are also different: HyPer-3 is monomeric, similar to HyPer. Therefore, HyPer-3 combines advantages of both previous versions (16). However, for an as yet unknown reason, HyPer-2 is brighter in mammalian cells than either HyPer or HyPer-3 (unpublished observations). All versions have equal quantum yields of 0.1, but differ in their extinction coefficients at 490 nm: 17.000 M^{-1} cm^{-1} (HyPer and HyPer-3) and 25.000 M^{-1} cm^{-1} (HyPer-2) (16). Therefore, HyPer-2 is the probe of choice for weakly expressing cells.

A form of HyPer with the combined mutations, Ala406Val and His34Tyr, was also created. This biosensor maintained the same high dynamic range as HyPer-2 and HyPer-3, but differs from both in exhibiting extremely long half-reduction and half-oxidation times (Fig. 2A, B). For this reason, HyPer-Ala406Val-His34Tyr cannot be used for real-time imaging, but could be potentially used as a memory biosensor for H_2O_2 (16) because of its prolonged oxidized state after stimulation, making it similar to turn-on synthetic ROS probes. This approach may allow determining, even after a long time after the stimulus, which cells in culture or tissue responded by H_2O_2 increase.

SypHer—best control for HyPer

Due to the structural characteristics of the chromophore, HyPer is sensitive to pH changes. Changes in pH lead to changes in chromophore protonation state. pH sensitivity is typical for many green fluorescent protein (GFP)-like proteins (25, 55, 92). However, the cpYFP and all sensors based on it are extremely sensitive to physiological pH changes. The fluorescence intensity of cpYFP (pK_a 8.6 with a 485 nm excitation) (189) is much more sensitive to intracellular pH changes than EYFP (pK_a 7.1) (126). HyPer as a chimeric protein $OxyR_{reg.domain}$-cpYFP with pK_a 8.6 at 490 nm and is not an exception from this rule. Acidification of the environment produces an increase in the intensity of the excitation peak at 420 nm and a decrease at 500 nm, which imitates reduction of HyPer (11, 163). Alkalization leads to the opposite effect.

Molecular mechanisms underlying spectral changes in response to oxidation or pH changes are not completely understood. However, some conclusions can be made. Both oxidation and alkalization increase probability of the deprotonated state of the Tyr phenol in the chromophore. This leads to increase of 500 nm excitation peak corresponding to deprotonated chromophore and proportional decrease of 400 nm excitation peak that belongs to the protonated form of

the chromophore. However, conformation changes caused by oxidation/reduction do not merely lead to changes in protonation state. As yet unknown changes in chromophore surroundings upon oxidation lead to (i) decrease in fluorescence lifetime and (ii) several fold increase in deprotonated chromophore extinction (16). What kind of intramolecular interactions are responsible for these changes is still to be resolved.

It is a well-known fact that during many physiological and pathological processes, the pH value may change, and sometimes significantly. Therefore, it is essential to use valid pH control in each experiment with HyPer.

Previously, to confirm the activity of OxyR in HyPer, the functional amino acid residue, Cys-199, was replaced by Ser199. HyPer-C199S does not respond to H_2O_2 and imitates fully reduced HyPer, thus demonstrating the key role of this Cys in the mechanism of the HyPer response to H_2O_2 (11). However, HyPer and HyPer-C199S have the same pH sensitivity with identical values of pK_a. HyPer-C199S was subsequently introduced as good pH sensor and received a new name, SypHer (163). It has been extensively characterized and used for imaging of pH changes in different compartments of living cells (163). SypHer has spectral properties similar to HyPer, thus both biosensors may be used in parallel experiments at the same settings. Some other pH indicators can also be used, including fluorescent dyes (89) and GFP-based indicators (12, 19). However, SypHer that differs only by single mutation and has identical spectral characteristics in comparison with HyPer is the most optimal pH control molecule for all versions of HyPer based on cpYFP in any systems.

HyPer-Red

Most of the widely used single-fluorophore biosensors have green fluorescence. Due to their spectral overlaps, these sensors cannot be imaged in the same system simultaneously. However, it is desirable to be able to detect several different parameters in one cell or tissue using sensors with different spectral characteristics. Moreover, biological tissues are poorly permeable to violet and blue excitation light as well as emitted green light. Therefore, there is considerable demand for the development of red fluorescent biosensors.

HyPer-Red, a red fluorescent version of the biosensor, was developed using green fluorescent HyPer as a template (59). The cpYFP in HyPer was replaced by a circularly permuted version of the red fluorescent protein mApple that has been used previously as the fluorescent domain of the Ca^{2+} indicator, R-GECO1 (225). HyPer-Red is an intensiometric biosensor: it has one excitation peak with a maximum at 575 nm and an emission peak at 605 nm. The sensitivity of HyPer-Red is similar to the other versions of HyPer based on cpYFP (59). The kinetic parameters of oxidation of HyPer-Red are comparable with other HyPer versions. The reaction rate constant is 3×10^5 $M^{-1}s^{-1}$ for HyPer-Red (59) compared with 5×10^5 $M^{-1}s^{-1}$, 1.2×10^5 $M^{-1}s^{-1}$, and 2.5×10^5 $M^{-1}s^{-1}$ for HyPer, HyPer-2, and HyPer-3, respectively (16). The reduction half-time of HyPer-Red is similar to that of HyPer-2 (59). Therefore, HyPer-Red enables the detection of even the low physiological amounts of H_2O_2 produced in cells by signaling cascades activated by growth factor stimulation, although the dynamic range of HyPer-Red is $\sim$30% lower compared with HyPer (59).

H_2O_2-insensitive version of HyPer-Red with the replacement of key cysteine residue has also been created for monitoring of pH changes in a parallel experiment. At the same time, pH titration profiles in the presence of nigericin and monensin of HyPer-Red and HyPer in the cytoplasm of eukaryotic cells are almost identical (59). Therefore, HyPerRed can now be used in multiparameter imaging settings in combination with SypHer, and similarly, HyPerRed-C199S can be expressed in the same cells together with yellow HyPer versions to serve as a pH control. Key properties of all HyPer versions are summarized in Table 1.

Various Imaging Techniques for HyPer

Confocal systems and widefield fluorescence microscopy are commonly used approaches for HyPer imaging. All examples described above obtained results using these devices. The two excitation peaks for HyPer permit its use in a ratiometric mode, in which the HyPer fluorescence is detected in separate channels, F_{420} and F_{500}, corresponding to excitation of the biosensor at 420 and 500 nm. The F_{500}/F_{420} ratio is the preferred signal of HyPer. Although the use of the ratiometric

Table 1. A Comparison of the HyPer Probe Properties

Characteristics	*HyPer*	*HyPer-2*	*HyPer-3*	*HyPer-Red*
Excitation maxima	420, 500 nm			575 nm
Emission maximum	516 nm			605 nm
Readout	ratio of fluorescence intensities excited at 500 and 420 nm (F_{500}/F_{420})			fluorescence intensity (F_{516})
Dynamic range	3 ± 0.4-fold	6 ± 0.3-fold	6 ± 0.3-fold	2 ± 0.2-fold
Oxidation rate constant (K_s), $M^{-1}\cdot sec^{-1}$	5×10^5	1.2×10^5	2.5×10^5	3.0×10^5
$[H_2O_2]$ at the half-maximal (K_{ox}) reaction rate	160 n*M*	290 n*M*	260 n*M*	140 n*M*
Sensitivity to H_2O_2 for the isolated probe	20–30 n*M*	20–30 n*M*	20–30 n*M*	20–30 n*M*
pK_a	8.6	8.6	8.6	8.7
QY	0.1	0.1	0.1	0.29
Brightness	1700	2500	1700	11,300
Oligomeric state at the 0.02 mg·mL^{-1} concentration	monomer	dimer	monomer	N/A
Reference	(11)	(131)	(16)	(59)

mode of HyPer is the preferred approach, single-wavelength imaging is also possible. However, the ratiometric readout avoids artifacts associated with different expression levels of the biosensor, cell movement, or changes in cellular shape. Ratiometric two-photon excitation has also successfully been applied to HyPer (214).

Recently, HyPer has found applications in fluorescence lifetime imaging microscopy (FLIM) (16). FLIM provides several advantages such as (i) the possibility of using a single excitation band for a single probe, (ii) independence from the expression level of the probe, (iii) quantitative readout, and (iv) much less interference from light scattering or photobleaching. Experiments with HyPer revealed that the fluorescence lifetimes of single-fluorophore biosensors significantly change upon activation. Previously, one example of single-fluorophore FLIM was demonstrated for pH-driven lifetime changes in enhanced green fluorescent protein (EGFP) (150). The fluorescence of HyPer and HyPer-3 excited at 488 nm increased upon H_2O_2 addition, while the lifetime decreased. HyPer-3 exhibited more pronounced changes in the fluorescence lifetime upon oxidation.

The lifetimes of oxidized and reduced HyPer differ enough to be suitable for H_2O_2 detection using FLIM even *in vivo*. In particular, the ability to detect the generation of H_2O_2 using FLIM after wounding of zebrafish larvae fins was tested using HyPer-3. The fluorescence lifetime changes in HyPer-3 distinctly showed a gradient of H_2O_2, with higher concentrations at the wounding site of the injured animals consistent with the results obtained by fluorescence imaging (Fig. 3) (16). Note that in all GFP variants tested (108, 150, 187), fluorescence lifetime either does not change or it increases with alkalization of the medium. Therefore, decrease in lifetime of HyPer-3 close to the wounding site is yet another argument for the existence of H_2O_2 gradient.

HyPer uses from a single live cell and its compartments to whole organisms

One of the main advantages of all genetically encoded biosensors is the ability to use them in living systems, both at the cellular level and at the level of the whole organism. This is possible due to the protein nature of these indicators. Each biosensor is encoded by a single gene that can be expressed in a tissue-specific manner in transgenic organisms. The protein nature of the biosensors allows them to be localized to various subcellular structures by adding a targeting sequence to the biosensor. Within a few years after its development, HyPer was used in many biological models with various levels of complexity, as shown in Table 2.

HyPer in cells and cellular organelles

The fluorescent signal of HyPer localized to various compartments, including the cytoplasm and nucleus (11, 129), mitochondrial matrix (11, 102, 129, 208), mitochondrial intermembrane space (129), and peroxisomes (43, 56, 129), significantly changes after extracellular addition of H_2O_2 and slightly when the same cells were exposed to the reducing compound, dithiothreitol (DTT) (129). This fact indicates that the HyPer in these compartments is in an almost completely reduced state. The most reduced state of HyPer was observed in the nucleus (129), whereas the most oxidized state was found in the lumen of the endoplasmic reticulum (ER) (58, 129), where more than 70% of HyPer is oxidized (129).

The ER is one of the most oxidized cellular compartments. Many proteins, including secreted and plasma membrane-associated proteins, have disulfide bonds that stabilize their structures and are necessary for normal function. The oxidizing environment of the ER is optimal for the formation of disulfide bonds of proteins (191). However, for HyPer, whether its oxidized state results from the high redox potential of the ER lumen or from high H_2O_2 production within this compartment remains unknown. The redox potential of the redox-active Cys-199-Cys-208 pair in wild-type OxyR is −185 mV (227). The homologous region of HyPer has the same potential. The glutathione redox potential in the ER measured by different approaches could range from −170 to −208 mV (17, 49, 100). For this reason, HyPer should be more than 50% reduced even in the highly oxidizing ER environment in the absence of H_2O_2. Therefore, we tend to think that both the low glutathione redox potential and intrinsic H_2O_2 production are responsible for HyPer oxidation in the ER.

Experimental studies have confirmed that the oxidized state of ER-localized HyPer reflects general oxidizing conditions inside this compartment in a greater degree than generation of H_2O_2 (138). The evidence was provided by the fact that overexpression of the H_2O_2-inactivating enzymes,

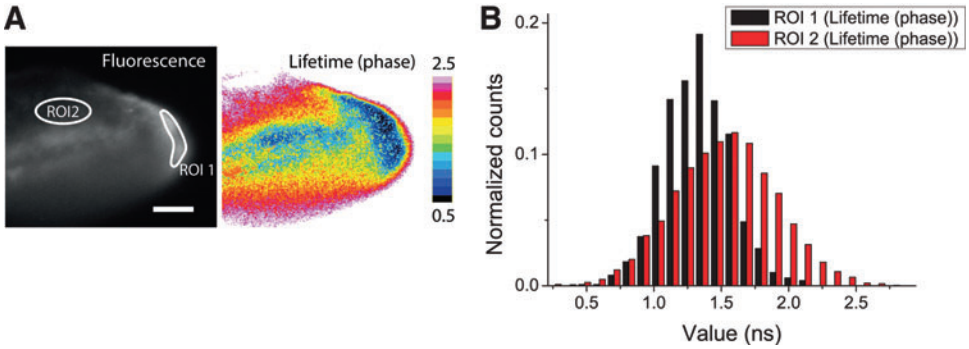

FIG. 3. Inflammation-driven H_2O_2 production in zebrafish larvae imaged using fluorescence lifetime imaging microscopy (FLIM) of HyPer-3 [Reprinted with permission from Bilan *et al.*, (16)]. **(A)** *Left* and *right panels* represent fluorescence intensity and FLIM images, respectively. ROI1 highlights the wound margin; ROI2 represents an area distant from the wound. **(B)** Fluorescence lifetime distribution plot for ROI1 and ROI2 in panel **(A)**. To see this illustration in color, the reader is referred to the web version of this article at www.liebertpub.com/ars

Table 2. Biological Systems Where HyPer Has Been Used

Cells		*Cell compartments*		*Organisms*	
Bacterial cells		Cytoplasm	(2, 9, 11, 13, 16, 32, 35, 36, 41, 58–60, 62, 73–75, 80, 83, 84, 88, 98, 101–105, 111, 115–117, 129, 131, 132, 141, 142, 145, 148, 149, 151, 158, 162, 168, 174, 179, 180, 185, 186, 201, 207, 213, 214, 220, 222, 224)	Fungi	
Escherichia coli	(11, 28, 59, 106, 123, 124)			*Cochliobolus heterostrophus*	(182)
Mammalian cell types					
Embryonic cells	(18, 59, 129, 141, 142, 145, 174, 199)				
Epithelial cells	(2, 21, 36, 101, 129, 215)	Mitochondrial matrix	(11, 13, 30, 36, 42, 46, 50, 56, 58, 59, 70, 74, 78, 83, 84, 88, 101, 102, 105, 109, 113, 115, 129, 154, 158, 163, 171, 180, 181, 194, 199, 201, 206–208, 214, 220, 224)	*Podospora anserina*	(216)
Endothelial cells	(9, 30, 62, 73, 103, 104, 115, 133, 208, 213, 220)			Plants	
Fibroblasts	(11, 70, 88, 129, 131, 138, 144, 145, 147, 148, 206, 207)			*Arabidopsis thaliana*	(14, 20, 43, 61, 95)
Muscle cells	(32, 41, 60, 80, 113, 151, 162, 171, 186, 224)	Mitochondrial intermembrane space	(59, 129)		
Neuronal cells	(84, 149, 168, 179, 214)	Nucleus	(2, 58, 88, 129, 158, 215)	*Medicago truncatula*	(3)
Hepatocytes	(74, 201)	Endoplasmic reticulum	(13, 17, 18, 58, 129, 135, 138, 174, 220)	Animals	
Islet cells	(56, 83, 181, 185)			*Caenorhabditis elegans*	(8, 29, 110, 212)
Preadipocytes	(180)	Peroxisomes	(21, 56, 75, 129)	*Danio rerio*	(16, 47, 57, 90, 153, 160, 161, 192, 221, 223)
T helper cells	(144)			*Xenopus laevis*	(127)
Cancer cell lines	(11, 13, 16, 17, 35, 42, 46, 51, 56, 58, 59, 70, 75, 78, 84, 98, 102, 105, 109, 111, 116, 117, 129, 131, 132, 138, 141, 145, 147, 154, 158, 163, 194, 222)	Membrane targeted	(58, 133, 144, 147)		

Numbers in the table correspond to the numbers of the references.

GPx and catalase, did not affect the fluorescent signal of ER-HyPer (138). Previous studies demonstrated that HyPer in other cellular compartments such as cytoplasm, mitochondria, and peroxisomes in catalase-overexpressing cells was significantly reduced in comparison with the control cells (56, 75, 83), and even the overexpression of the ER-resident antioxidant enzyme, peroxiredoxin IV (204, 205), did not affect the ER-HyPer redox state (138). However, in other studies, ER-HyPer has been successfully used. For example, H_2O_2 transportation into the lumen of ER *via* aquaporin-8 was investigated using HyPer (13). In summary, it should be noted that the oxidized state of HyPer in the ER is maintained mainly because of low reducing power of this compartment rather than the high level of H_2O_2.

Targeted HyPer allows the investigation of the dynamics of low concentrations of H_2O_2 in the various compartments in the physiological settings (Table 2), including treatment of cells with PDGF or tumor necrosis factor alpha (TNF-α) or the inhibition of the mitochondrial electron transport chain (129).

HyPer-cyto is the most widely used version of the available HyPer derivatives. In this case, the biosensor easily diffuses within the nucleocytoplasmic compartment. Production of H_2O_2 during stimulation of cells with growth factors such as epidermal growth factor (EGF) (132, 141), PDGF (131), and nerve growth factor (NGF) (11) was first visualized using this version. In addition, HyPer is also suitable for use in other cellular models.

The results of redox-proteomic studies revealed that the average level of the protein thiol oxidation in various cellular compartments is the same. However, the degree to which the protein thiol groups involved in different signaling pathways are oxidized can vary significantly even within a single compartment (77). Therefore, the oxidation processes in the cellular compartments can occur locally, which suggests that during some signaling events, ROS are also produced locally. HyPer has been successfully used for imaging such local sites of H_2O_2 production (144, 146, 147).

It is known that stimulation of cells with EGF causes EGF receptor (EGFR) internalization (69), an increase of Ca^{2+} in the cytoplasm (27) and production of H_2O_2 in low concentrations (132). By fusing HyPer with different membrane-associated proteins, the biosensor has been immobilized on the cytoplasmic surfaces of plasma membrane, endosomes, and the ER membrane. Upon activation of tyrosine kinase cascades, H_2O_2 microdomains were visualized by the membrane-localized HyPer (146, 147). HyPer fused to EGF receptor (EGFR) showed specific H_2O_2 production on the cytoplasmic surface of the endosomes. Upon stimulation of the cells with EGF, the EGFR-HyPer fusion was internalized into the endosomes. HyPer on the surface of the endosomes started to be oxidized after internalization. At the same time, the noninternalized EGRF-HyPer remained reduced, demonstrating that (i) H_2O_2 was produced locally; (ii) no H_2O_2 production was associated with the plasma membrane; and (iii) H_2O_2 diffusion from the endosomes to the plasma membrane did not occur (Fig. 4).

Similarly, HyPer has been immobilized on the cytoplasmic side of the ER membrane. This enabled the detection of the microdomain of H_2O_2 near the phosphatase PTP-1B (147). These experiments directly demonstrated for the first time that H_2O_2 acts locally under physiological conditions.

Insulin induces several signaling cascades, including Ca^{2+} release from intracellular stores, and enhances the production of ROS in different cell types. HyPer has been used for studies of insulin-stimulated ROS production in myotubes. HyPer detected the increase in H_2O_2 in the cytoplasm of the myotubes after insulin stimulation. However, incubation of the myotubes with a specific inhibitor of $p47^{phox}$-dependent NADPH oxidase, apocynin, prevented this increase. Thus, it became clear that insulin caused generation of H_2O_2 due to NADPH oxidase activation (60). In another study, generation of H_2O_2 was shown in cultures of primary neurons after high-frequency electrical stimulation. Electrical stimulation of neuronal cells enhances Ca^{2+}-dependent H_2O_2 generation *via* stimulation of a neuronal NADPH oxidase activity (179).

It is known that cell death is accompanied by active generation of ROS, including H_2O_2. HyPer is the most appropriate tool for visualization of this phenomenon. HyPer was used to visualize the H_2O_2 changes in the cytosol and

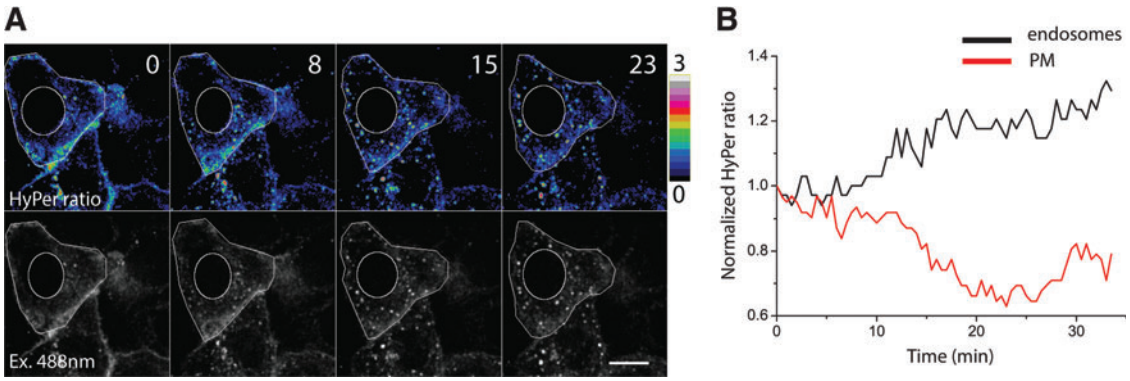

FIG. 4. Microdomains of elevated H_2O_2 generation upon activation of epidermal growth factor receptor (EGFR) [Reprinted with permission from Mishina *et al.*, (147)]. **(A)** Confocal images of EGFR-HyPer-expressing HeLa-Kyoto cells at indicated time points (in minutes) after stimulation of the cells with 50 ng/ml EGF. *Upper row* of images represents subcellular distribution of HyPer ratio. *Lower row* of images shows subcellular distribution of EGFR-HyPer. Cell boundaries and nucleus of one of the cells are highlighted. Scale bar: 15 μm. **(B)** Time course of H_2O_2 production associated with endosomes and plasma membrane in the cells shown in **(A)**. To see this illustration in color, the reader is referred to the web version of this article at www.liebertpub.com/ars

mitochondria of HeLa cells exposed to the apoptogenic protein, Apo2L/TRAIL. Changes in the mitochondrial transmembrane potential were measured in parallel using the dye, tetramethylrhodamine methyl ester (TMRM). Together with the decrease in the transmembrane potential and changes of the cell shape, the cytosolic and mitochondrial H_2O_2 levels increased during cell degradation upon stimulation with Apo2L/TRAIL (11).

HyPer-Red was successfully used in multiparameter imaging to solve the controversy regarding whether the H_2O_2 level in the mitochondrial matrix changes as a function of the Ca^{2+} load. The data obtained earlier using isolated mitochondria supported opposite views (54, 87, 93, 112, 114, 196). For this reason, HyPer-Red was cotransfected into human embryonic kidney (HEK) cells in different combinations with different green-emitting biosensors for pH, H_2O_2, and the GSH/GSSG ratio targeted to various compartments (59). It was demonstrated that inducing ER stress by inhibiting the Ca^{2+} uptake by the ER leads to a transient increase in the mitochondrial level of H_2O_2 (Fig. 5). An alternative method to increase mitochondrial Ca^{2+}, inducing ATP-evoked Ca^{2+} release, did not cause any detectible H_2O_2 changes. Coexpression of mito-HyPer-Red with a green HyPer version targeted to the cytoplasm or to the mitochondrial intermembrane space revealed a highly localized spatial distribution of H_2O_2 restricted to the matrix. The increase in H_2O_2 was not associated with a change in the GSH/GSSG ratio (59). In the future, HyPer-Red could be combined in different experimental setups with other biosensors, including green-emitting HyPers, NAD^+/NADH indicators (15, 99, 226), rxYFP (156), and roGFPs (52, 85, 91), for GSSG/2GSH registration and others.

HyPer can be used in bacteria as well as in eukaryotic cells (28, 124). The minimum concentration of exogenous H_2O_2

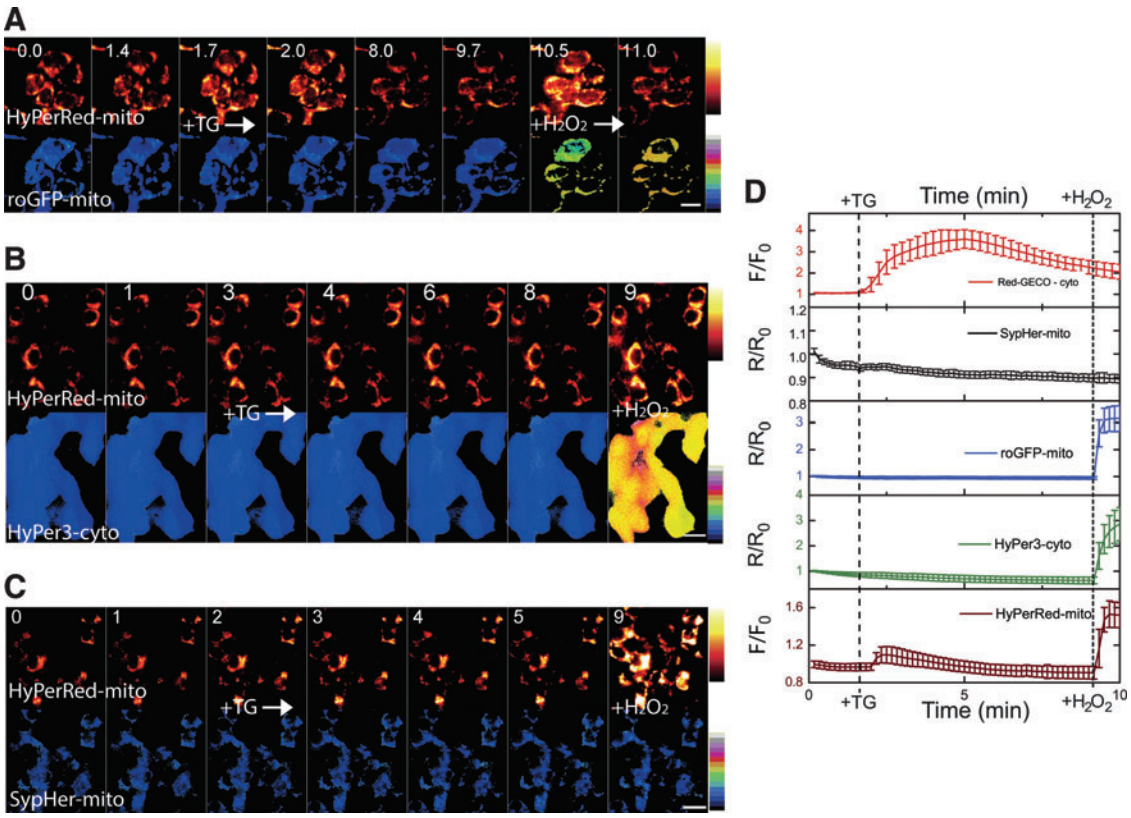

FIG. 5. Multiparameter imaging of H_2O_2, GSH/GSSG, Ca^{2+}, and pH [Reprinted with permission from Ermakova *et al.*, (59)]. **(A)** Inhibition of SERCA Ca^{2+} pump by thapsigargin (TG) induces temporal H_2O_2 increase in the mitochondrial matrix, whereas the GSH/GSSG ratio remains unchanged. HEK-293 cells were cotransfected with HyPerRed-mito (*upper row*) and roGFP-mito (*lower row*). *Numbers* indicate timing in minutes. Scale bar, 20 μm. *Lookup tables* indicate HyPerRed brightness (3700–25,000, 16 bit scale) and the roGFP-mito ratio (0.5–4). **(B)** H_2O_2 does not spread from the mitochondria to the cytoplasm of the cells. HEK-293 cells were cotransfected with HyPerRed-mito (*upper row*) and HyPer3-cyto (*lower row*). *Numbers* indicate timing in minutes. Scale bar, 30 μm. *Lookup tables* indicate HyPerRed brightness (3700–25,000, 16 bit scale) and HyPer-3 ratio (0.5–6). **(C)** Mitochondrial pH remains stable upon SERCA Ca^{2+} pump inhibition and matrix H_2O_2 release. HEK-293 cells were cotransfected with HyPerRed-mito (*upper row*) and SypHer-mito (*lower row*). *Numbers* indicate timing in minutes. Scale bar, 40 μm. *Lookup tables* indicate HyPerRed brightness (3700–25,000, 16 bit scale) and SypHer ratio (0.5–4). **(D)** TG induces temporal H_2O_2 increase in the mitochondrial matrix (measured using HyPerRed-mito), while cytosolic H_2O_2 (HyPer3-cyto), mitochondrial GSH/GSSG (roGFP-mito), and mitochondrial pH (SypHer-mito) remain stable. In each experiment, HyPerRed-mito was coexpressed with either HyPer3-cyto or roGFP-mito or SypHer-mito. The panel shows values ± SDs for more than 100 cells in two or more experiments for each sensor combination. The agonist was added at the 1.7-min time point. For sample images, see panels **(A–C)**. To see this illustration in color, the reader is referred to the web version of this article at www.liebertpub.com/ars

for detectable changes in the HyPer fluorescence in a suspension of *E. coli* cells is 5 μM (11). Later studies characterized in detail the HyPer responses in *E. coli* exposed to external H_2O_2. These recent studies are very important for understanding the role of H_2O_2 in the immunological response of higher organisms against pathogenic bacteria and are also useful for evaluating the general quantitative performance of the biosensor (124). HyPer also has been used in the study, demonstrating that enhancing endogenous ROS production makes bacteria more susceptible to oxidative stress and antibiotic activity (28). In another study, HyPer was used as an efficient readout for improvement of H_2O_2-producing function of cytochrome P450 variants (123).

HyPer is suitable for studies on the roles of H_2O_2 in most cellular models, and combinations with other sensors enable multiparameter imaging in single live cells. Due to the high rate of reaction of HyPer with H_2O_2 (the rate constant is $\sim 10^5$ $M^{-1}s^{-1}$) (16), the biosensor has a very high temporal resolution: this fact is very important for any biosensor-based imaging of fast messenger or activity fluctuations. However, this characteristic raises the question of whether HyPer could function as an antioxidant enzyme peroxidase. This seems unlikely because the peroxiredoxin-like antioxidant activity of an enzyme requires not only a fast oxidation rate but also very rapid reduction by electron-supplying enzymes such as thioredoxin and glutathione/glutaredoxin systems. This is, for example, the case for AhpC peroxidase in *E. coli* cells (38, 159, 165, 167). By contrast, bacteria evolved OxyR and scientists later produced HyPer as oxidant-sensing molecules. These molecules have high oxidation rates, but much slower reduction rates (5, 16), which make them more useful as sensors than as antioxidants. In the systems in which HyPer had been used *in vivo*, there were no inhibitory effects of HyPer on redox-dependent physiological reactions, whereas external antioxidants or Nox inhibitors had dramatic effects (90, 127, 153). Examples of such uses are provided below.

However, the main problem in studies using HyPer is the pH sensitivity of the biosensor. Without the adequate pH control, the fluorescent changes of HyPer may lead to misinterpretation of the results. Many of the above examples, including stimulation of cells with different growth factors (11, 60, 131, 132, 141, 179), were conducted without such controls. Although later experiments with the pH indicator, SypHer, proved that some growth factors such as PDGF and EGF do not cause pH changes in the cytoplasm, in other cases, such as apoptosis or inhibition of the respiratory chain, intracellular pH may vary significantly. For HyPer localized in cellular compartments, pH control should also be performed in the same compartment.

HyPer in vivo

Until recently, there was no information regarding the role of H_2O_2 in paracrine signaling. This was first demonstrated in the model of zebrafish *Danio rerio* larvae that were wounded by cutting their tail fins (153). Zebrafish larvae are commonly used for investigations of inflammatory and regenerative processes in vertebrate organisms. Upon injury of the tail fins of the zebrafish larvae at 3 days postfertilization, HyPer indicated tissue-scale gradients of H_2O_2 at the wound area (Fig. 6).

The H_2O_2 can reach concentrations of 0.5–50 μM near the wound margin with a 100–200 μm gradient from the margin into the epithelium. The gradient was observed beginning 3 min after wounding and reached a maximum at 20 min. These estimated concentrations of H_2O_2 were obtained by calibration of HyPer. For this, the fins of the zebrafish larvae expressing HyPer were exposed to increasing exogenous H_2O_2. Using the same settings for each imaging series, the

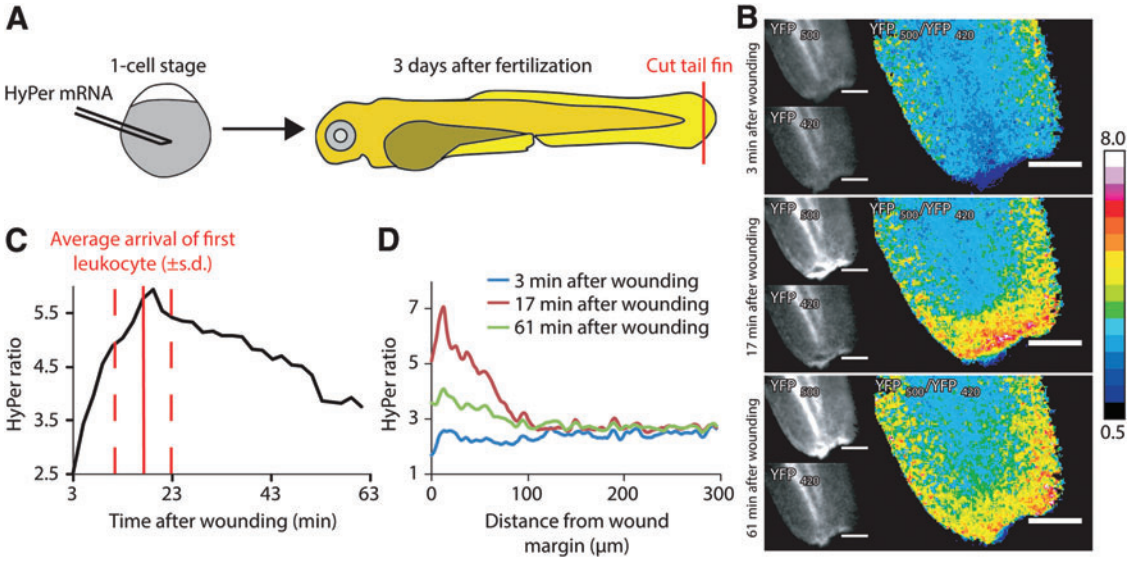

FIG. 6. Wound margin H_2O_2 production in zebrafish larvae [Reprinted with permission from Niethammer *et al.*, (153)]. (A) Experimental procedure. **(B)** HyPer imaging in an injured zebrafish larva. [H_2O_2] is inferred from the YFP_{500}/YFP_{420} excitation ratio of HyPer. Grayscale scaling is adjusted to improve contrast. Pseudocolor calibration bars: HyPer ratio (YFP_{500}/YFP_{420}). Scale bars: 100 μm. **(C)** Temporal [H_2O_2] profile in a $\sim$10–30-μm broad region of interest along the wound margin. Arrival of first leukocyte at wound (*solid red line*) ± SD (*dashed red line*) is shown. **(D)** [H_2O_2] line profile normal to the wound margin. To see this illustration in color, the reader is referred to the web version of this article at www.liebertpub.com/ars

HyPer ratio then may be transformed into H_2O_2 concentration. However, in the estimation of H_2O_2 levels in the tissue using external calibration, the authors did not make a correction for H_2O_2 gradient across the plasma membrane, which could range from 200 to 600-fold. Therefore, the real numbers for the H_2O_2 concentration in the wounded fin are most probably within the 5–200 n*M* range, which is more realistic given the low level of molecular oxygen in the animal tissues.

The gradient of H_2O_2 was necessary for leukocyte recruitment to the wound (153). Previously, a chemotactic effect of H_2O_2 had been shown *in vitro* for some types of cells (107, 121). However, this was the first demonstration of this effect in an *in vivo* model. Notably, the H_2O_2 production in the wound area preceded the recruitment of leukocytes (153). The observations in this study indicate that generation of H_2O_2 during the inflammatory response is not associated with the activity of leukocytes as previously thought (190). The dual oxidase (Duox) is responsible for creating this gradient of H_2O_2 in the area of wound. Specific inhibition of Duox significantly reduces the H_2O_2 production in the fin after wounding. Furthermore, it strongly attenuates the migration of the leukocytes into the region of inflammation (153). The gradient of H_2O_2 in this model was also observed using an improved version of the biosensor, HyPer-3 (16).

The authors did not use SypHer as a control, but instead used YFP and 2′,7′-Bis-(2-Carboxyethyl)-5-(and-6)-Carboxyfluorescein, both having smaller dynamic range compared with SypHer. However, there are data to suggest that the gradient of HyPer ratio is indeed determined by H_2O_2, at least to a large extent. First, the gradient of H_2O_2 in this model was also observed using an improved version of the biosensor, HyPer-3 (16). Notably, HyPer-3 pH titration profile is identical to that of HyPer, unlike the dynamic range of H_2O_2 response, which is 2-fold higher in HyPer-3. HyPer-3 ratio change upon wounding is elevated compared with that of HyPer, meaning substantial contribution of H_2O_2 to this signal change. Moreover, the direction of fluorescence lifetime response (decrease) of HyPer-3 in the wound model strongly supports the existence of H_2O_2 gradient (see details in the Various imaging techniques for HyPer section).

In further studies, HyPer has been specifically expressed in the neutrophils of zebrafish larvae. The experiments demonstrated that the arriving neutrophils dissipate the gradient of H_2O_2 in the region of wound by means of myeloperoxidase (160).

Interesting results were obtained in transgenic *Xenopus laevis* that expressed HyPer (127). *Xenopus* tadpole tail amputation also induces pronounced H_2O_2 production similar to that in *D. rerio*. Notably, the concentration of H_2O_2 remained high (50–200 μM) at the injury site for several days after the amputation of the tail, until the completion of the wound healing (Fig. 7). Inhibition of the NADPH oxidases and addition of therapeutic antioxidants reduced the H_2O_2 level. However, reducing the level of H_2O_2 significantly impaired the regeneration dynamics of the tails after wounding, as indicated by the shorter lengths of the tails. Thus, H_2O_2 is an important regulator of tissue regeneration. It is already known that an increased level of H_2O_2 activates the Wnt/β-catenine signaling pathway during regeneration (127).

In *Xenopus*, addition of antioxidants blocked the regeneration, whereas expression of HyPer in the tissue did not. Therefore, this study also confirms that HyPer cannot be considered as an effective antioxidant. pH monitoring in this study (127) was carried out using a pH-sensitive FP, pHluorin (140), which confirmed the specificity of the HyPer response during processes of tadpole tale regeneration (127).

Zebrafish are a good model system in which to study organ regeneration due to their strong regenerative potential.

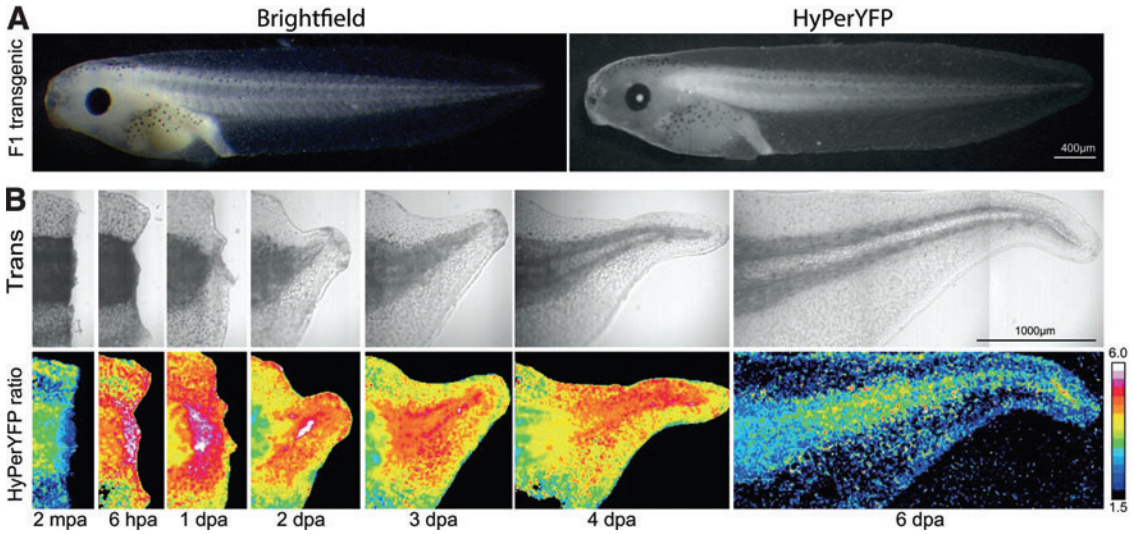

FIG. 7. Production of reactive oxygen species (ROS) during Xenopus tadpole tail regeneration [Reprinted with permission from Love *et al.*, (127)]. **(A)** Bright-field and fluorescence micrographs of a tadpole derived from the F1 generation of a transgenic *Xenopus laevis* line that expresses the H_2O_2 sensor HyPerYFP ubiquitously. **(B)** HyPer transillumination (Trans) imaging of a representative regenerating tadpole tail. [H_2O_2] is derived from the excitation ratio of HyPerYFP490nm/HyPerYFP402 nm. mpa, minutes postamputation; hpa, hours postamputation; dpa, days postamputation. Owing to the size of the regenerated tail, the 6 dpa time point panels are derived from the merging of three images. Pseudocolor calibration bars: HyPer ratio. To see this illustration in color, the reader is referred to the web version of this article at www.liebertpub.com/ars

Therefore, they are often used as the organism of choice for cardiac regeneration studies (81, 169, 175). HyPer imaging in the hearts of adult zebrafish revealed increases in the H_2O_2 levels in the epicardium and the adjacent myocardium at the resection site after organ injury. The high H_2O_2 level was maintained during the cardiac regeneration processes and returned to its basal level only after the full recovery of the injured heart. Interestingly, in contrast to rapid inflammatory H_2O_2 response in zebrafish larvae tail fins after wounding, the H_2O_2 production induced by injury to the heart is slower. Decreasing the H_2O_2 level during the regeneration processes by using NADPH oxidase inhibitors or by catalase overexpression in the tissues significantly impaired the cardiac regeneration. These valuable data further confirm an important role for H_2O_2 in regeneration mechanisms (90).

Oxidative stress and therefore ROS are involved in aging processes. It has been shown that oxidative damage of various cellular molecules increases with age (64). HyPer has been used in a study designed to investigate the role of ROS in the life span of *Caenorhabditis elegans*, a well-established eukaryotic aging model (8, 110). HyPer demonstrated a significant increase in the H_2O_2 level in the body of *C. elegans* with age. Interestingly, a dietary restriction that prolongs life span of worms delayed H_2O_2 elevation (8). Moreover, local regions with high H_2O_2 concentration were identified using HyPer in young adult individuals. For example, canal-associated neurons and hypodermal syncytium, hyp7, have the most elevated levels of H_2O_2 (8). Experiments with SypHer as a pH control in this study have not been done. Adding this control to the study would be important as the intestine of nematodes becomes slightly acidified during aging (8). pH changes may occur in other tissues especially upon perturbations of metabolism.

In another study, the H_2O_2 levels at different developmental stages of the worm were determined by independent approaches: by monitoring the thiol redox status of different proteins using a quantitative redox proteomic technique and using HyPer and Amplex UltraRed for intra- and extracellular H_2O_2 monitoring, respectively. All of these methods showed that at early stages of development, the animals accumulate high levels of H_2O_2, whereas in adulthood, the concentrations of H_2O_2 are significantly lower. As aging starts, the H_2O_2 level again begins to increase. Changes in the general cellular redox environment during the development of *C. elegans* were confirmed by a quantitative redox proteomic technique. This approach allows quantitative determination of the redox states of protein thiol groups at different time points in the life span of the animals. The proteome of *C. elegans* is more oxidized at the initial stages of development and during aging; these results are consistent with the data obtained for H_2O_2 using HyPer. Overall, the results obtained in these studies suggest that cellular redox changes at the initial stages in life may determine the life span (110).

HyPer may also be used to investigate the role of H_2O_2 in plants and even in the different compartments of plant cells (43, 61, 95). First, experiments with HyPer in plants demonstrated H_2O_2 dynamics *in vivo* in plant peroxisomes (43). HyPer used together with the Ca^{2+} biosensor, D3cpv (157), also targeted to plant peroxisomes, confirmed the modulation of H_2O_2 by Ca^{2+} signaling. The intraperoxisomal Ca^{2+} elevation following the rise in the cytoplasm significantly accelerated H_2O_2 scavenging due to the stimulation of catalase activity in this compartment (43). In Arabidopsis roots exposed to aluminum, HyPer was used to monitor intracellular H_2O_2 changes. It was shown that in the elongation zone of roots, the H_2O_2 level significantly decreases after aluminum treatment (95). However, the mechanisms by which aluminum inhibits root elongation are poorly understood. Effect of possible pH changes on HyPer was not verified in this study and therefore cannot be excluded.

Plant cells constantly produce different types of ROS as by-products during photosynthesis. In fact, exposure of photosynthetic cells to high light intensities leads to the strong accumulation of ROS, including H_2O_2, in chloroplasts, which can cause intracellular oxidative damage (71, 202). Using HyPer, it was demonstrated that upon exposure to high doses of light, even nonphotosynthetic cotyledon epidermal cells produce H_2O_2 in Arabidopsis (61). However, these interesting results have to be confirmed by the reliable control experiments concerning the determination of possible pH changes.

HyPer with Combined Functions

Development of biosensors with dual functions is another interesting approach to multiplexing the readouts in multiparameter imaging. Such biosensors allow detection of two independent parameters at the same time by means of two independent readouts.

PH domains fused to FPs are often used for visualization of phosphorylated forms of phosphatidylinositol (PI) (209). One such domain, the PH domain from Bruton's tyrosine kinase (BTK), is specifically sensitive to phosphatidylinositol 3,4,5-trisphosphate (PIP3) (144) and redistributes from the cytoplasm to the plasma membrane upon PI3-kinase activation. Fusing HyPer with BTK-PH resulted in a probe named PIP-SHOW (PIP3 and SH Oxidation Watching) that senses both PIP3 and H_2O_2 by translocation and ratiometric readouts, respectively. The biosensor moves to the cellular plasma membrane after an increase in PIP3, which is a clear indication of phosphatidylinositol 3-kinase (PI3K) activity. The biosensor F_{500}/F_{420} ratio reports the changes in the concentration of H_2O_2.

A single probe with these dual functions was tested in NIH 3T3 fibroblasts stimulated with PDGF. After cell stimulation, the translocation of the probe to the plasma membrane indicates PI3K activation, and the ratiometric fluorescent signal changes indicate the production of H_2O_2. PIP-SHOW was used to study the lipid and redox signaling events of the first phase of CD4+ human T helper (T_H) cell activation. For this purpose, PIP-SHOW was expressed in human T_H cells. Addition of beads coated with anti-CD3/CD28 to T_H cells led to the formation of immunological synapses between the cells and the beads. Within these contacts, which were stable throughout the experiment, a strong local increase in the PIP3 level and rapid generation of H_2O_2 were reported using the PIP-SHOW sensor (Fig. 8) (144). This combined sensor shows how easy and efficient it is to combine readouts within a single probe. Indeed, instead of HyPer, any other ratiometric probe (for Ca^{2+}, pH, NAD^+/NADH, *etc.*) can be used. In a complementary manner, BTK-PH can be replaced with any domain that translocates within the cell upon activation or inhibition of signaling or metabolic activities.

H_2O_2 generation and detection using DAO and HyPer

Recently, HyPer was fused with the yeast D-amino acid oxidase (DAO) (134), to produce an efficient H_2O_2 generator/

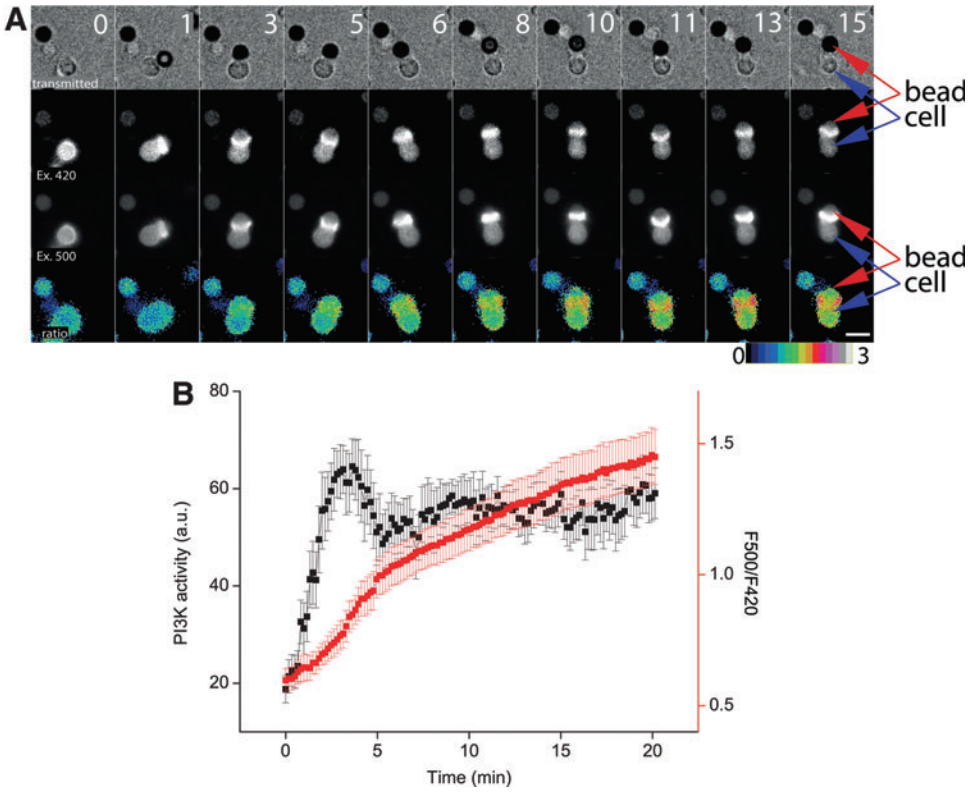

FIG. 8. PIP-SHOW detects PI3K activity and H_2O_2 production in the human T helper (T_H) cell upon formation of the immunological synapse [Reprinted with permission from Mishina *et al.*, (144)]. **(A)** Widefield fluorescence images of T_H cell forming a contact with anti-CD3/CD28-coated beads (added at time point zero). *Numbers* indicate time points in minutes. *Upper row* of the images represents transmitted light channel (beads are *dense black*); two next *lower rows* show distribution of the fluorescence sequentially excited at 420 and 505 nm; *lowest row* represents distribution of H_2O_2 represented by the 505/420 excitation ratio. Scale bar: 10 μm. **(B)** Mean values of PI3K activity and H_2O_2 production in 28 T_H cells from three experiments and two donors. Error bars indicate standard error of mean. To see this illustration in color, the reader is referred to the web version of this article at www.liebertpub.com/ars

detector system. DAO oxidizes the NH_2- group of D-amino acids to produce α-keto acids, ammonia, and H_2O_2 (120, 164). DAO can be thus used as a controllable source of H_2O_2 in cells. The activity of the expressed enzyme in cells may be controlled using external additions of D-alanine as the substrate for DAO (94). Because in mammalian cells all of the amino acids are in the L-optical isoform (with rare exceptions), D-alanine is a specific substrate for DAO, and in the absence of D-Ala, no H_2O_2 is produced. The DAO/HyPer fusion protein allows the determination of the dynamics of H_2O_2 production and the sensitivity to externally added D-alanine in the living cells. Intracellular visualization of DAO activity revealed heterogeneity in the dynamics of H_2O_2 production among individual cells. This finally answered the question of how much H_2O_2 is produced by DAO in mammalian cells. As it turned out, even with a millimolar excess of added D-alanine, the concentration of H_2O_2 produced by DAO in cells does not exceed 50–100 n*M* (134).

Conclusions

The H_2O_2 molecule is a relatively short-lived but important cellular regulator. Many adverse roles of ROS, including cell-damaging effects, have been attributed to this molecule as well as to other ROS (1, 64). Subsequently, the roles of ROS were reconsidered due to the accumulated evidence for specific and reversible redox regulation of cellular processes. A change in the viewpoint regarding ROS led to many important discoveries. In particular, it is currently known that different cells produce H_2O_2 themselves as a second messenger for signaling pathways. Many reviews have been devoted to various functions of H_2O_2 (53, 65, 66, 72, 82, 176, 193, 197, 210). Currently, this molecule is of great interest to investigators in the field of redox biology.

However, studies of redox regulation and oxidative stress are impossible without accessible and reliable methods. Initially, various dyes were the main tools for *in vitro* studies of ROS. This approach was far from perfect and helped to answer a limited number of questions. Unfortunately, hundreds of articles were produced using improper methodologies of ROS detection, which are therefore difficult to interpret (22, 130, 183, 184).

The discovery of FPs has opened substantial opportunities for investigation of biological events in living organisms. FP-based genetically encoded biosensors have, for the first time, allowed specific real-time visualization of cellular processes, including redox events. HyPer for detection of H_2O_2 level was one of the first redox biosensors (11). Today, HyPer is an effective tool for studying the role of H_2O_2 in the fine regulation of both cellular signaling and oxidative stress. Over the past few years, this biosensor has been widely used in many biological models from organelles to whole organisms. The

high demand and widespread use of the HyPer family of biosensors are probably the best proof of their effectiveness. The main advantage of HyPer as a biosensor lies in its protein nature that allows it to be expressed in all types of cells and even with specific localizations within the cell. It can also be combined with other readouts. Because OxyR is a bacterial protein, HyPer has no known interaction partners in eukaryotic cells except the thiol reduction cellular systems that enable its reduction. Expression of HyPer is therefore nontoxic for cells, which reduces the likelihood of false signals.

An important question for HyPer relates to its possible antioxidant role because it reacts with H_2O_2 and thus neutralizes the oxidant. However, in most cases, including *in vivo* tests, HyPer has demonstrated no effect on the H_2O_2-dependent physiological processes. An effect of the peroxidase activity of HyPer was detected only once in the experimental model, *Arabidopsis thaliana* (14). However, in principle, this problem cannot be totally excluded for other models. This concern exists not only for HyPer but also for other redox biosensors (128). Another issue relates to the pH dependence of HyPer, which can be solved by using pH biosensor, SypHer, as a control (11, 163). In many experiments, HyPer has been used without monitoring of pH changes. However, the side-by-side use of pH controls is an essential condition for any research involving HyPer.

HyPer has considerable future potential. There is substantial interest in the use of HyPer to study the roles of H_2O_2 in mammals *in vivo*. It is therefore necessary to develop brighter variants of the biosensor. This will be possible with the development of new circular permutants of other FPs. Versions of HyPer with different spectral characteristics will allow them to be combined with each other or with other biosensors within a single cell.

Many indisputable advantages and the incredible flexibility of the genetically encoded biosensors have made HyPer a key tool for redox biology investigators.

Acknowledgments

This work was supported by a Russian Science Foundation grant 14-14-00747 and COST action ''EU-ROS.'' Research on DAOs was supported by a Russian Foundation for Basic research grant 15-34-20805.

Author Disclosure Statement

No competing financial interests exist.

References

1. Adler V, Yin Z, Tew KD, and Ronai Z. Role of redox potential and reactive oxygen species in stress signaling. *Oncogene* 18: 6104–6111, 1999.
2. Ameziane-El-Hassani R, Boufraqech M, Lagente-Chevallier O, Weyemi U, Talbot M, Métivier D, Courtin F, Bidart JM, El Mzibri M, Schlumberger M, and Dupuy C. Role of H_2O_2 in RET/PTC1 chromosomal rearrangement produced by ionizing radiation in human thyroid cells. *Cancer Res* 70: 4123–4132, 2010.
3. Andrio E, Marino D, Marmeys A, de Segonzac MD, Damiani I, Genre A, Huguet S, Frendo P, Puppo A, and Pauly N. Hydrogen peroxide-regulated genes in the *Medicago truncatula*-Sinorhizobium meliloti symbiosis. *New Phytol* 198: 179–189, 2013.
4. Arnér ES and Holmgren A. Physiological functions of thioredoxin and thioredoxin reductase. *Eur J Biochem* 267: 6102–6109, 2000.
5. Aslund F, Zheng M, Beckwith J, and Storz G. Regulation of the OxyR transcription factor by hydrogen peroxide and the cellular thiol-disulfide status. *Proc Natl Acad Sci U S A* 96: 6161–6165, 1999.
6. Babior BM, Kipnes RS, and Curnutte JT. Biological defense mechanisms. The production by leukocytes of superoxide, a potential bactericidal agent. *J Clin Invest* 52: 741–744, 1973.
7. Babior BM, Lambeth JD, and Nauseef W. The neutrophil NADPH oxidase. *Arch Biochem Biophys* 397: 342–344, 2002.
8. Back P, De Vos WH, Depuydt GG, Matthijssens F, Vanfleteren JR, and Braeckman BP. Exploring real-time in vivo redox biology of developing and aging *Caenorhabditis elegans*. *Free Radic Biol Med* 52: 850–859, 2012.
9. Barroso M, Florindo C, Kalwa H, Silva Z, Turanov AA, Carlson BA, de Almeida IT, Blom HJ, Gladyshev VN, Hatfield DL, Michel T, Castro R, Loscalzo J, and Handy DE. Inhibition of cellular methyltransferases promotes endothelial cell activation by suppressing glutathione peroxidase 1 protein expression. *J Biol Chem* 289: 15350–15362, 2014.
10. Bedard K and Krause KH. The NOX family of ROS-generating NADPH oxidases: physiology and pathophysiology. *Physiol Rev* 87: 245–313, 2007.
11. Belousov VV, Fradkov AF, Lukyanov KA, Staroverov DB, Shakhbazov KS, Terskikh AV, and Lukyanov S. Genetically encoded fluorescent indicator for intracellular hydrogen peroxide. *Nat Methods* 3: 281–286, 2006.
12. Benčina M. Illumination of the spatial order of intracellular pH by genetically encoded pH-sensitive sensors. *Sensors (Basel)* 13: 16736–16758, 2013.
13. Bertolotti M, Bestetti S, García-Manteiga JM, Medraño-Fernandez I, Dal Mas A, Malosio ML, and Sitia R. Tyrosine kinase signal modulation: a matter of H_2O_2 membrane permeability? *Antioxid Redox Signal* 19: 1447–1451, 2013.
14. Bieker S, Riester L, Stahl M, Franzaring J, and Zentgraf U. Senescence-specific alteration of hydrogen peroxide levels in *Arabidopsis thaliana* and oilseed rape spring variety Brassica napus L. cv. Mozart. *J Integr Plant Biol* 54: 540–554, 2012.
15. Bilan DS, Matlashov ME, Gorokhovatsky AY, Schultz C, Enikolopov G, and Belousov VV. Genetically encoded fluorescent indicator for imaging NAD(+)/NADH ratio changes in different cellular compartments. *Biochim Biophys Acta* 1840: 951–957, 2014.
16. Bilan DS, Pase L, Joosen L, Gorokhovatsky AY, Ermakova YG, Gadella TW, Grabher C, Schultz C, Lukyanov S, and Belousov VV. HyPer-3: a genetically encoded H_2O_2 probe with improved performance for ratiometric and fluorescence lifetime imaging. *ACS Chem Biol* 8: 535–542, 2013.
17. Birk J, Meyer M, Aller I, Hansen HG, Odermatt A, Dick TP, Meyer AJ, and Appenzeller-Herzog C. Endoplasmic reticulum: reduced and oxidized glutathione revisited. *J Cell Sci* 126: 1604–1617, 2013.
18. Birk J, Ramming T, Odermatt A, and Appenzeller-Herzog C. Green fluorescent protein-based monitoring of endoplasmic reticulum redox poise. *Front Genet* 4: 108, 2013.
19. Bizzarri R, Serresi M, Luin S, and Beltram F. Green fluorescent protein based pH indicators for in vivo use: a review. *Anal Bioanal Chem* 393: 1107–1122, 2009.
20. Boisson-Dernier A, Lituiev DS, Nestorova A, Franck CM, Thirugnanarajah S, and Grossniklaus U. ANXUR receptor-like kinases coordinate cell wall integrity with growth at the

pollen tube tip via NADPH oxidases. *PLoS Biol* 11: e1001719, 2013.
21. Bonekamp NA, Sampaio P, de Abreu FV, Lüers GH, and Schrader M. Transient complex interactions of mammalian peroxisomes without exchange of matrix or membrane marker proteins. *Traffic* 13: 960–978, 2012.
22. Bonini MG, Rota C, Tomasi A, and Mason RP. The oxidation of 2′,7′-dichlorofluorescin to reactive oxygen species: a self-fulfilling prophesy? *Free Radic Biol Med* 40: 968–975, 2006.
23. Bouloumié A, Bauersachs J, Linz W, Schölkens BA, Wiemer G, Fleming I, and Busse R. Endothelial dysfunction coincides with an enhanced nitric oxide synthase expression and superoxide anion production. *Hypertension* 30: 934–941, 1997.
24. Boveris A. Mitochondrial production of superoxide radical and hydrogen peroxide. *Adv Exp Med Biol* 78: 67–82, 1977.
25. Brejc K, Sixma TK, Kitts PA, Kain SR, Tsien RY, Ormo M, and Remington SJ. Structural basis for dual excitation and photoisomerization of the Aequorea victoria green fluorescent protein. *Proc Natl Acad Sci U S A* 94: 2306–2311, 1997.
26. Bretón-Romero R and Lamas S. Hydrogen peroxide signaling in vascular endothelial cells. *Redox Biol* 2: 529–534, 2014.
27. Bryant JA, Finn RS, Slamon DJ, Cloughesy TF, and Charles AC. EGF activates intracellular and intercellular calcium signaling by distinct pathways in tumor cells. *Cancer Biol Ther* 3: 1243–1249, 2004.
28. Brynildsen MP, Winkler JA, Spina CS, MacDonald IC, and Collins JJ. Potentiating antibacterial activity by predictably enhancing endogenous microbial ROS production. *Nat Biotechnol* 31: 160–165, 2013.
29. Cabreiro F, Ackerman D, Doonan R, Araiz C, Back P, Papp D, Braeckman BP, and Gems D. Increased life span from overexpression of superoxide dismutase in *Caenorhabditis elegans* is not caused by decreased oxidative damage. *Free Radic Biol Med* 51: 1575–1582, 2011.
30. Casellato A, Rossi Paccani S, Barrile R, Bossi F, Ciucchi L, Codolo G, Pizza M, Aricò B, and de Bernard M. The C2 fragment from Neisseria meningitidis antigen NHBA increases endothelial permeability by destabilizing adherens junctions. *Cell Microbiol* 16: 925–937, 2014.
31. Chance B, Sies H, and Boveris A. Hydroperoxide metabolism in mammalian organs. *Physiol Rev* 59: 527–605, 1979.
32. Chang KH, Park JM, and Lee MY. Feasibility of simultaneous measurement of cytosolic calcium and hydrogen peroxide in vascular smooth muscle cells. *BMB Rep* 46: 600–605, 2013.
33. Chelikani P, Fita I, and Loewen PC. Diversity of structures and properties among catalases. *Cell Mol Life Sci* 61: 192–208, 2004.
34. Chen K, Thomas SR, and Keaney JF Jr. Beyond LDL oxidation: ROS in vascular signal transduction. *Free Radic Biol Med* 35: 117–132, 2003.
35. Chen P, Stone J, Sullivan G, Drisko JA, and Chen Q. Anticancer effect of pharmacologic ascorbate and its interaction with supplementary parenteral glutathione in preclinical cancer models. *Free Radic Biol Med* 51: 681–687, 2011.
36. Cheng WY, Larson JM, and Samet JM. Monitoring intracellular oxidative events using dynamic spectral unmixing microscopy. *Methods* 66: 345–352, 2014.
37. Choi H, Kim S, Mukhopadhyay P, Cho S, Woo J, Storz G, and Ryu SE. Structural basis of the redox switch in the OxyR transcription factor. *Cell* 105: 103–113, 2001.
38. Christman MF, Morgan RW, Jacobson FS, and Ames BN. Positive control of a regulon for defenses against oxidative stress and some heat-shock proteins in *Salmonella typhimurium*. *Cell* 41: 753–762, 1985.
39. Claiborne A, Miller H, Parsonage D, and Ross RP. Protein-sulfenic acid stabilization and function in enzyme catalysis and gene regulation. *FASEB J* 7: 1483–1490, 1993.
40. Collet JF and Messens J. Structure, function, and mechanism of thioredoxin proteins. *Antioxid Redox Signal* 13: 1205–1216, 2010.
41. Contreras-Ferrat A, Llanos P, Vásquez C, Espinosa A, Osorio-Fuentealba C, Arias-Calderon M, Lavandero S, Klip A, Hidalgo C, and Jaimovich E. Insulin elicits a ROS-activated and an IP_3-dependent Ca^{2+} release, which both impinge on GLUT4 translocation. *J Cell Sci* 127: 1911–1923, 2014.
42. Corazao-Rozas P, Guerreschi P, Jendoubi M, André F, Jonneaux A, Scalbert C, Garçon G, Malet-Martino M, Balayssac S, Rocchi S, Savina A, Formstecher P, Mortier L, Kluza J, and Marchetti P. Mitochondrial oxidative stress is the Achille's heel of melanoma cells resistant to Braf-mutant inhibitor. *Oncotarget* 4: 1986–1998, 2013.
43. Costa A, Drago I, Behera S, Zottini M, Pizzo P, Schroeder JI, Pozzan T, and Lo Schiavo F. H_2O_2 in plant peroxisomes: an in vivo analysis uncovers a Ca(2+)-dependent scavenging system. *Plant J* 62: 760–772, 2010.
44. Cross AR and Segal AW. The NADPH oxidase of professional phagocytes—prototype of the NOX electron transport chain systems. *Biochim Biophys Acta* 1657: 1–22, 2004.
45. Crow JP. Dichlorodihydrofluorescein and dihydrorhodamine 123 are sensitive indicators of peroxynitrite in vitro: implications for intracellular measurement of reactive nitrogen and oxygen species. *Nitric Oxide* 1: 145–157, 1997.
46. Csordás G, Golenár T, Seifert EL, Kamer KJ, Sancak Y, Perocchi F, Moffat C, Weaver D, de la Fuente Perez S, Bogorad R, Koteliansky V, Adijanto J, Mootha VK, and Hajnóczky G. MICU1 controls both the threshold and cooperative activation of the mitochondrial Ca^{2+} uniporter. *Cell Metab* 17: 976–987, 2013.
47. Deng Q, Harvie EA, and Huttenlocher A. Distinct signalling mechanisms mediate neutrophil attraction to bacterial infection and tissue injury. *Cell Microbiol* 14: 517–528, 2012.
48. Denu JM and Tanner KG. Specific and reversible inactivation of protein tyrosine phosphatases by hydrogen peroxide: evidence for a sulfenic acid intermediate and implications for redox regulation. *Biochemistry* 37: 5633–5642, 1998.
49. Dixon BM, Heath SH, Kim R, Suh JH, and Hagen TM. Assessment of endoplasmic reticulum glutathione redox status is confounded by extensive ex vivo oxidation. *Antioxid Redox Signal* 10: 963–972, 2008.
50. Dong LF, Jameson VJ, Tilly D, Cerny J, Mahdavian E, Marín-Hernández A, Hernández-Esquivel L, Rodríguez-Enríquez S, Stursa J, Witting PK, Stantic B, Rohlena J, Truksa J, Kluckova K, Dyason JC, Ledvina M, Salvatore BA, Moreno-Sánchez R, Coster MJ, Ralph SJ, Smith RA, and Neuzil J. Mitochondrial targeting of vitamin E succinate enhances its pro-apoptotic and anti-cancer activity via mitochondrial complex II. *J Biol Chem* 286: 3717–3728, 2011.
51. Dong LF, Jameson VJ, Tilly D, Prochazka L, Rohlena J, Valis K, Truksa J, Zobalova R, Mahdavian E, Kluckova K, Stantic M, Stursa J, Freeman R, Witting PK,Norberg E, Goodwin J, Salvatore BA, Novotna J, Turanek J, Ledvina M, Hozak P, Zhivotovsky B, Coster MJ, Ralph SJ, Smith RA, and Neuzil J. Mitochondrial targeting of α-tocopheryl succinate enhances its pro-apoptotic efficacy: a new paradigm for effective cancer therapy. *Free Radic Biol Med* 50: 1546–1555, 2011.

52. Dooley CT, Dore TM, Hanson GT, Jackson WC, Remington SJ, and Tsien RY. Imaging dynamic redox changes in mammalian cells with green fluorescent protein indicators. *J Biol Chem* 279: 22284–22293, 2004.
53. Droge W. Free radicals in the physiological control of cell function. *Physiol Rev* 82: 47–95, 2002.
54. Dykens JA. Isolated cerebral and cerebellar mitochondria produce free radicals when exposed to elevated CA2+ and Na+: implications for neurodegeneration. *J Neurochem* 63: 584–591, 1994.
55. Elsliger MA, Wachter RM, Hanson GT, Kallio K, and Remington SJ. Structural and spectral response of green fluorescent protein variants to changes in pH. *Biochemistry* 38: 5296–5301, 1999.
56. Elsner M, Gehrmann W, and Lenzen S. Peroxisome-generated hydrogen peroxide as important mediator of lipotoxicity in insulin-producing cells. *Diabetes* 60: 200–208, 2011.
57. Enyedi B and Niethammer P. H_2O_2: a chemoattractant? *Methods Enzymol* 528: 237–255, 2013.
58. Enyedi B, Varnai P, and Geiszt M. Redox state of the endoplasmic reticulum is controlled by Ero1L-alpha and intraluminal calcium. *Antioxid Redox Signal* 13: 721–729, 2010.
59. Ermakova YG, Bilan DS, Matlashov ME, Mishina NM, Markvicheva KN, Subach OM, Subach FV, Bogeski I, Hoth M, Enikolopov G, and Belousov VV. Red fluorescent genetically encoded indicator for intracellular hydrogen peroxide. *Nat Commun* 5: 5222, 2014.
60. Espinosa A, Garcia A, Hartel S, Hidalgo C, and Jaimovich E. NADPH oxidase and hydrogen peroxide mediate insulin-induced calcium increase in skeletal muscle cells. *J Biol Chem* 284: 2568–2575, 2009.
61. Exposito-Rodriguez M, Laissue PP, Littlejohn GR, Smirnoff N, and Mullineaux PM. The use of HyPer to examine spatial and temporal changes in H_2O_2 in high light-exposed plants. *Methods Enzymol* 527: 185–201, 2013.
62. Feine I, Pinkas I, Salomon Y, and Scherz A. Local oxidative stress expansion through endothelial cells—a key role for gap junction intercellular communication. *PLoS One* 7: e41633, 2012.
63. Fernandes AP and Holmgren A. Glutaredoxins: glutathione-dependent redox enzymes with functions far beyond a simple thioredoxin backup system. *Antioxid Redox Signal* 6: 63–74, 2004.
64. Finkel T and Holbrook NJ. Oxidants, oxidative stress and the biology of ageing. *Nature* 408: 239–247, 2000.
65. Finkel T. Signal transduction by reactive oxygen species in non-phagocytic cells. *J Leukoc Biol* 65: 337–340, 1999.
66. Finkel T. Signal transduction by reactive oxygen species. *J Cell Biol* 194: 7–15, 2011.
67. Flohe L, Günzler WA, and Schock HH. Glutathione peroxidase: a selenoenzyme. *FEBS Lett* 32: 132–134, 1973.
68. Freitas M, Lima JL, and Fernandes. Optical probes for detection and quantification of neutrophils' oxidative burst. *Anal Chim Acta* 649: 8–23, 2009.
69. Futter CE, Pearse A, Hewlett LJ, and Hopkins CR. Multivesicular endosomes containing internalized EGF-EGF receptor complexes mature and then fuse directly with lysosomes. *J Cell Biol* 132: 1011–1023, 1996.
70. Galimov ER, Chernyak BV, Sidorenko AS, Tereshkova AV, and Chumakov PM. Prooxidant properties of p66shc are mediated by mitochondria in human cells. *PLoS One* 9: e86521, 2014.
71. Galvez-Valdivieso G and Mullineaux PM. The role of reactive oxygen species in signalling from chloroplasts to the nucleus. *Physiol Plant* 138: 430–439, 2010.
72. Gamaley IA and Klyubin IV. Roles of reactive oxygen species: signaling and regulation of cellular functions. *Int Rev Cytol* 188: 203–255, 1999.
73. Gandhirajan RK, Meng S, Chandramoorthy HC, Mallilankaraman K, Mancarella S, Gao H, Razmpour R, Yang XF, Houser SR, Chen J, Koch WJ, Wang H, Soboloff J, Gill DL, and Madesh M. Blockade of NOX2 and STIM1 signaling limits lipopolysaccharide-induced vascular inflammation. *J Clin Invest* 123: 887–902, 2013.
74. Gaspers LD, Mémin E, and Thomas AP. Calcium-dependent physiologic and pathologic stimulus-metabolic response coupling in hepatocytes. *Cell Calcium* 52: 93–102, 2012.
75. Gehrmann W and Elsner M. A specific fluorescence probe for hydrogen peroxide detection in peroxisomes. *Free Radic Res* 45: 501–506, 2011.
76. Giannoni E, Buricchi F, Raugei G, Ramponi G, and Chiarugi P. Intracellular reactive oxygen species activate Src tyrosine kinase during cell adhesion and anchorage-dependent cell growth. *Mol Cell Biol* 25: 6391–6403, 2005.
77. Go YM, Duong DM, Peng J, and Jones DP. Protein cysteines map to functional networks according to steady-state level of oxidation. *J Proteomics Bioinform* 4: 196–209, 2012.
78. Gogvadze V, Norberg E, Orrenius S, and Zhivotovsky B. Involvement of Ca2+ and ROS in alpha-tocopheryl succinate-induced mitochondrial permeabilization. *Int J Cancer* 127: 1823–1832, 2010.
79. Gomes A, Fernandes E, and Lima JL. Fluorescence probes used for detection of reactive oxygen species. *J Biochem Biophys Methods* 65: 45–80, 2005.
80. González-Ramos M, Mora I, de Frutos S, Garesse R, Rodríguez-Puyol M, Olmos G, and Rodríguez-Puyol D. Intracellular redox equilibrium is essential for the constitutive expression of AP-1 dependent genes in resting cells: studies on TGF-β1 regulation. *Int J Biochem Cell Biol* 44: 963–971, 2012.
81. Gonzalez-Rosa JM, Martin V, Peralta M, Torres M, and Mercader N. Extensive scar formation and regression during heart regeneration after cryoinjury in zebrafish. *Development* 138: 1663–1674, 2011.
82. Groeger G, Quiney C, and Cotter TG. Hydrogen peroxide as a cell-survival signaling molecule. *Antioxid Redox Signal* 11: 2655–2671, 2009.
83. Gurgul-Convey E, Mehmeti I, Lortz S, and Lenzen S. Cytokine toxicity in insulin-producing cells is mediated by nitro-oxidative stress-induced hydroxyl radical formation in mitochondria. *J Mol Med (Berl)* 89: 785–798, 2011.
84. Gusdon AM, Zhu J, Van Houten B, and Chu CT. ATP13A2 regulates mitochondrial bioenergetics through macroautophagy. *Neurobiol Dis* 45: 962–972, 2012.
85. Gutscher M, Pauleau AL, Marty L, Brach T, Wabnitz GH, Samstag Y, Meyer AJ, and Dick TP. Real-time imaging of the intracellular glutathione redox potential. *Nat Methods* 5: 553–559, 2008.
86. Gutscher M, Sobotta MC, Wabnitz GH, Ballikaya S, Meyer AJ, Samstag Y, and Dick TP. Proximity-based protein thiol oxidation by H_2O_2-scavenging peroxidases. *J Biol Chem* 284: 31532–31540, 2009.
87. Gyulkhandanyan AV and Pennefather PS. Shift in the localization of sites of hydrogen peroxide production in brain mitochondria by mitochondrial stress. *J Neurochem* 90: 405–421, 2004.

88. Hajas G, Bacsi A, Aguilera-Aguirre L, Hegde ML, Tapas KH, Sur S, Radak Z, Ba X, and Boldogh I. 8-Oxoguanine DNA glycosylase-1 links DNA repair to cellular signaling via the activation of the small GTPase Rac1. *Free Radic Biol Med* 61: 384–394, 2013.
89. Han J and Burgess K. Fluorescent indicators for intracellular pH. *Chem Rev* 110: 2709–2728, 2010.
90. Han P, Zhou XH, Chang N, Xiao CL, Yan S, Ren H, Yang XZ, Zhang ML, Wu Q, Tang B, Diao JP, Zhu X, Zhang C, Li CY, Cheng H, and Xiong JW. Hydrogen peroxide primes heart regeneration with a derepression mechanism. *Cell Res* 24: 1091–1107, 2014.
91. Hanson GT, Aggeler R, Oglesbee D, Cannon M, Capaldi RA, Tsien RY, and Remington SJ. Investigating mitochondrial redox potential with redox-sensitive green fluorescent protein indicators. *J Biol Chem* 279: 13044–13053, 2004.
92. Hanson GT, McAnaney TB, Park ES, Rendell ME, Yarbrough DK, Chu S, Xi L, Boxer SG, Montrose MH, and Remington SJ. Green fluorescent protein variants as ratiometric dual emission pH sensors. 1. Structural characterization and preliminary application. *Biochemistry* 41: 15477–15488, 2002.
93. Hansson MJ, Månsson R, Morota S, Uchino H, Kallur T, Sumi T, Ishii N, Shimazu M, Keep MF, Jegorov A, and Elmér E. Calcium-induced generation of reactive oxygen species in brain mitochondria is mediated by permeability transition. *Free Radic Biol Med* 45: 284–294, 2008.
94. Haskew-Layton RE, Payappilly JB, Smirnova NA, Ma TC, Chan KK, Murphy TH, Guo H, Langley B, Sultana R, Butterfield DA, Santagata S, Alldred MJ, Gazaryan IG, Bell GW, Ginsberg SD, and Ratan RR. Controlled enzymatic production of astrocytic hydrogen peroxide protects neurons from oxidative stress via an Nrf2-independent pathway. *Proc Natl Acad Sci U S A* 107: 17385–17390, 2010.
95. Hernández-Barrera A, Velarde-Buendía A, Zepeda I, Sanchez F, Quinto C, Sánchez-Lopez R, Cheung AY, Wu HM, and Cardenas L. Hyper, a hydrogen peroxide sensor, indicates the sensitivity of the Arabidopsis root elongation zone to aluminum treatment. *Sensors (Basel)* 15: 855–867, 2015.
96. Hofmann B, Hecht HJ, and Flohé L. Peroxiredoxins. *Biol Chem* 383: 347–364, 2002.
97. Holmgren A. Thioredoxin structure and mechanism: conformational changes on oxidation of the active-site sulfhydryls to a disulfide. *Structure* 3: 239–243, 1995.
98. Huang BK and Sikes HD. Quantifying intracellular hydrogen peroxide perturbations in terms of concentration. *Redox Biol* 2: 955–962, 2014.
99. Hung YP, Albeck JG, Tantama M, and Yellen G. Imaging cytosolic NADH-NAD(+) redox state with a genetically encoded fluorescent biosensor. *Cell Metab* 14: 545–554, 2011.
100. Hwang C, Sinskey AJ, and Lodish HF. Oxidized redox state of glutathione in the endoplasmic reticulum. *Science* 257: 1496–1502, 1992.
101. Ishikawa F, Kaneko E, Sugimoto T, Ishijima T, Wakamatsu M, Yuasa A, Sampei R, Mori K, Nose K, and Shibanuma M. A mitochondrial thioredoxin-sensitive mechanism regulates TGF-β-mediated gene expression associated with epithelial-mesenchymal transition. *Biochem Biophys Res Commun* 443: 821–827, 2014.
102. Jiang J, Maeda A, Ji J, Baty CJ, Watkins SC, Greenberger JS, and Kagan VE. Are mitochondrial reactive oxygen species required for autophagy? *Biochem Biophys Res Commun* 412: 55–60, 2011.
103. Jin BY, Sartoretto JL, Gladyshev VN, and Michel T. Endothelial nitric oxide synthase negatively regulates hydrogen peroxide-stimulated AMP-activated protein kinase in endothelial cells. *Proc Natl Acad Sci U S A* 106: 17343–17348, 2009.
104. Kalwa H, Sartoretto JL, Sartoretto SM, and Michel T. Angiotensin-II and MARCKS: a hydrogen peroxide- and RAC1-dependent signaling pathway in vascular endothelium. *J Biol Chem* 287: 29147–29158, 2012.
105. Kaminskyy VO, Piskunova T, Zborovskaya IB, Tchevkina EM, and Zhivotovsky B. Suppression of basal autophagy reduces lung cancer cell proliferation and enhances caspase-dependent and -independent apoptosis by stimulating ROS formation. *Autophagy* 8: 1032–1044, 2012.
106. Kim E, Gordonov T, Liu Y, Bentley WE, and Payne GF. Reverse engineering to suggest biologically relevant redox activities of phenolic materials. *ACS Chem Biol* 8: 716–724, 2013.
107. Klyubin IV, Kirpichnikova KM, and Gamaley IA. Hydrogen peroxide-induced chemotaxis of mouse peritoneal neutrophils. *Eur J Cell Biol* 70: 347–351, 1996.
108. Kneen M, Farinas J, Li Y, and Verkman AS. Green fluorescent protein as a noninvasive intracellular pH indicator. *Biophys J* 74: 1591–1599, 1998.
109. Kniss A, Lu H, Jones DP, and Kemp ML. A microfluidic systems biology approach for live single-cell mitochondrial ROS imaging. *Methods Enzymol* 526: 219–230, 2013.
110. Knoefler D, Thamsen M, Koniczek M, Niemuth NJ, Diederich AK, and Jakob U. Quantitative in vivo redox sensors uncover oxidative stress as an early event in life. *Mol Cell* 47: 767–776, 2012.
111. Koczurkiewicz P, Podolak I, Skrzeczyńska-Moncznik J, Sarna M, Wójcik KA, Ryszawy D, Galanty A, Lasota S, Madeja Z, Czyż J, and Michalik M. Triterpene saponosides from *Lysimachia ciliata* differentially attenuate invasive potential of prostate cancer cells. *Chem Biol Interact* 206: 6–17, 2013.
112. Komary Z, Tretter L, and Adam-Vizi V. H_2O_2 generation is decreased by calcium in isolated brain mitochondria. *Biochim Biophys Acta* 1777: 800–807, 2008.
113. Korde AS, Yadav VR, Zheng YM, and Wang YX. Primary role of mitochondrial Rieske iron-sulfur protein in hypoxic ROS production in pulmonary artery myocytes. *Free Radic Biol Med* 50: 945–952, 2011.
114. Kowaltowski AJ, Castilho RF, and Vercesi AE. Ca(2+)-induced mitochondrial membrane permeabilization: role of coenzyme Q redox state. *Am J Physiol* 269: C141–C147, 1995.
115. Kozieł R, Pircher H, Kratochwil M, Lener B, Hermann M, Dencher NA, and Jansen-Dürr P. Mitochondrial respiratory chain complex I is inactivated by NADPH oxidase Nox4. *Biochem J* 452: 231–239, 2013.
116. Kratschmar DV, Calabrese D, Walsh J, Lister A, Birk J, Appenzeller-Herzog C, Moulin P, Goldring CE, and Odermatt A. Suppression of the Nrf2-dependent antioxidant response by glucocorticoids and 11β-HSD1-mediated glucocorticoid activation in hepatic cells. *PLoS One* 7: e36774, 2012.
117. Kruzel ML, Actor JK, Zimecki M, Wise J, Płoszaj P, Mirza S, Kruzel M, Hwang SA, Ba X, and Boldogh I. Novel recombinant human lactoferrin: differential activation of oxidative stress related gene expression. *J Biotechnol* 168: 666–675, 2013.
118. Lee C, Lee SM, Mukhopadhyay P, Kim SJ, Lee SC, Ahn WS, Yu MH, Storz G, and Ryu SE. Redox regulation of

OxyR requires specific disulfide bond formation involving a rapid kinetic reaction path. *Nat Struct Mol Biol* 11: 1179–1185, 2004.
119. Lee SR, Kwon KS, Kim SR, and Rhee SG. Reversible inactivation of protein-tyrosine phosphatase 1B in A431 cells stimulated with epidermal growth factor. *J Biol Chem* 273: 15366–15372, 1998.
120. Lee YH, and Chu WS. D-Amino acid oxidase activity form Rhodosporiduim toruloides. *Lett Appl Microbiol* 23: 283–286, 1996.
121. Li W, Liu G, Chou IN, and Kagan HM. Hydrogen peroxide-mediated, lysyl oxidase-dependent chemotaxis of vascular smooth muscle cells. *J Cell Biochem* 78: 550–557, 2000.
122. Lillig CH, Berndt C, and Holmgren A. Glutaredoxin systems. *Biochim Biophys Acta* 1780: 1304–1317, 2008.
123. Lim JB and Sikes HD. Use of a genetically encoded hydrogen peroxide sensor for whole cell screening of enzyme activity. *Protein Eng Des Sel* 28: 79–83, 2015.
124. Lim JB, Barker KA, Huang BK, and Sikes HD. In-depth characterization of the fluorescent signal of HyPer, a probe for hydrogen peroxide, in bacteria exposed to external oxidative stress. *J Microbiol Methods* 106: 33–39, 2014.
125. Liu H, Colavitti R, Rovira II, and Finkel T. Redox-dependent transcriptional regulation, *Circ Res* 97: 967–974, 2005.
126. Llopis J, McCaffery JM, Miyawaki A, Farquhar MG, and Tsien RY. Measurement of cytosolic, mitochondrial, and Golgi pH in single living cells with green fluorescent proteins. *Proc Natl Acad Sci U S A* 95: 6803–6808, 1998.
127. Love NR, Chen Y, Ishibashi S, Kritsiligkou P, Lea R, Koh Y, Gallop JL, Dorey K, and Amaya E. Amputation-induced reactive oxygen species are required for successful Xenopus tadpole tail regeneration. *Nat Cell Biol* 15: 222–228, 2013.
128. Lukyanov KA and Belousov VV. Genetically encoded fluorescent redox sensors. *Biochim Biophys Acta* 1840: 745–756, 2013.
129. Malinouski M, Zhou Y, Belousov VV, Hatfield DL, and Gladyshev VN. Hydrogen peroxide probes directed to different cellular compartments. *PLoS One* 6: e14564, 2011.
130. Marchesi E, Rota C, Fann YC, Chignell CF, and Mason RP. Photoreduction of the fluorescent dye 2′-7′-dichlorofluorescein: a spin trapping and direct electron spin resonance study with implications for oxidative stress measurements. *Free Radic Biol Med* 26: 148–161, 1999.
131. Markvicheva KN, Bilan DS, Mishina NM, Gorokhovatsky AY, Vinokurov LM, Lukyanov S, and Belousov VV. A genetically encoded sensor for H_2O_2 with expanded dynamic range. *Bioorg Med Chem* 19: 1079–1084, 2011.
132. Markvicheva KN, Bogdanova EA, Staroverov DB, Lukyanov S, and Belousov VV. Imaging of intracellular hydrogen peroxide production with HyPer upon stimulation of HeLa cells with epidermal growth factor. *Methods Mol Biol* 476: 79–86, 2008.
133. Martinelli R, Kamei M, Sage PT, Massol R, Varghese L, Sciuto T, Toporsian M, Dvorak AM, Kirchhausen T, Springer TA, and Carman CV. Release of cellular tension signals self-restorative ventral lamellipodia to heal barrier micro-wounds. *J Cell Biol* 201: 449–465, 2013.
134. Matlashov ME, Belousov VV, and Enikolopov G. How much H_2O_2 is produced by recombinant D-amino acid oxidase in mammalian cells? *Antioxid Redox Signal* 20: 1039–1044, 2014.
135. Matus S, Lopez E, Valenzuela V, Nassif M, and Hetz C. Functional contribution of the transcription factor ATF4 to the pathogenesis of amyotrophic lateral sclerosis. *PLoS One* 8: e66672, 2013.
136. McCord JM and Fridovich I. Superoxide dismutase. An enzymic function for erythrocuprein (hemocuprein). *J Biol Chem* 244: 6049–6055, 1969.
137. McCord JM and Fridovich I. The reduction of cytochrome c by milk xanthine oxidase. *J Biol Chem* 243: 5753–5760, 1968.
138. Mehmeti I, Lortz S, and Lenzen S. The H_2O_2-sensitive HyPer protein targeted to the endoplasmic reticulum as a mirror of the oxidizing thiol-disulfide milieu. *Free Radic Biol Med* 53: 1451–1458, 2012.
139. Meyer AJ and Dick TP. Fluorescent protein-based redox probes. *Antioxid Redox Signal* 13: 621–650, 2010.
140. Miesenböck G, De Angelis DA, and Rothman JE. Visualizing secretion and synaptic transmission with pH-sensitive green fluorescent proteins. *Nature* 394: 192–195, 1998.
141. Miller EW, Dickinson BC, and Chang CJ. Aquaporin-3 mediates hydrogen peroxide uptake to regulate downstream intracellular signaling. *Proc Natl Acad Sci U S A* 107: 15681–15686, 2010.
142. Miller EW, Taulet N, Onak CS, New EJ, Lanselle JK, Smelick GS, and Chang CJ. Light-activated regulation of cofilin dynamics using a photocaged hydrogen peroxide generator. *J Am Chem Soc* 132: 17071–17073, 2010.
143. Miller EW, Tulyathan O, Isacoff EY, and Chang CJ. Molecular imaging of hydrogen peroxide produced for cell signaling. *Nat Chem Biol* 3: 263–267, 2007.
144. Mishina NM, Bogeski I, Bolotin DA, Hoth M, Niemeyer BA, Schultz C, Zagaynova EV, Lukyanov S, and Belousov VV. Can we see PIP(3) and hydrogen peroxide with a single probe? *Antioxid Redox Signal* 17: 505–512, 2012.
145. Mishina NM, Markvicheva KN, Bilan DS, Matlashov ME, Shirmanova MV, Liebl D, Schultz C, Lukyanov S, and Belousov VV. Visualization of intracellular hydrogen peroxide with HyPer, a genetically encoded fluorescent probe. *Methods Enzymol* 526: 45–59, 2013.
146. Mishina NM, Markvicheva KN, Fradkov AF, Zagaynova EV, Schultz C, Lukyanov S, and Belousov VV. Imaging H_2O_2 microdomains in receptor tyrosine kinases signaling. *Methods Enzymol* 526: 175–187, 2013.
147. Mishina NM, Tyurin-Kuzmin PA, Markvicheva KN, Vorotnikov AV, Tkachuk VA, Laketa V, Schultz C, Lukyanov S, and Belousov VV. Does cellular hydrogen peroxide diffuse or act locally? *Antioxid Redox Signal* 14: 1–7, 2011.
148. Morinaka A, Funato Y, Uesugi K, and Miki H. Oligomeric peroxiredoxin-I is an essential intermediate for p53 to activate MST1 kinase and apoptosis. *Oncogene* 30: 4208–4218, 2011.
149. Morinaka A, Yamada M, Itofusa R, Funato Y, Yoshimura Y, Nakamura F, Yoshimura T, Kaibuchi K, Goshima Y, Hoshino M, Kamiguchi H, and Miki H. Thioredoxin mediates oxidation-dependent phosphorylation of CRMP2 and growth cone collapse. *Sci Signal* 4: ra26, 2011.
150. Nakabayashi T, Wang HP, Kinjo M, and Ohta N. Application of fluorescence lifetime imaging of enhanced green fluorescent protein to intracellular pH measurements. *Photochem Photobiol Sci* 7: 668–670, 2008.

151. Narayanan D, Xi Q, Pfeffer LM, and Jaggar JH. Mitochondria control functional CaV1.2 expression in smooth muscle cells of cerebral arteries. *Circ Res* 107: 631–641, 2010.
152. Nauseef WM. How human neutrophils kill and degrade microbes: an integrated view. *Immunol Rev* 219: 88–102, 2007.
153. Niethammer P, Grabher C, Look AT, and Mitchison TJ. A tissue-scale gradient of hydrogen peroxide mediates rapid wound detection in zebrafish. *Nature* 459: 996–999, 2009.
154. Norberg E, Gogvadze V, Vakifahmetoglu H, Orrenius S, and Zhivotovsky B. Oxidative modification sensitizes mitochondrial apoptosis-inducing factor to calpain-mediated processing. *Free Radic Biol Med* 48: 791–797, 2010.
155. Oakley FD, Abbott D, Li Q, and Engelhardt JF. Signaling components of redox active endosomes: the redoxosomes. *Antioxid Redox Signal* 11: 1313–1333, 2009.
156. Ostergaard H, Henriksen A, Hansen FG, and Winther JR. Shedding light on disulfide bond formation: engineering a redox switch in green fluorescent protein. *EMBO J* 20: 5853–5862, 2001.
157. Palmer AE, Giacomello M, Kortemme T, Hires SA, Lev-Ram V, Baker D, and Tsien RY. Ca2+ indicators based on computationally redesigned calmodulin-peptide pairs. *Chem Biol* 13: 521–530, 2006.
158. Panieri E, Gogvadze V, Norberg E, Venkatesh R, Orrenius S, and Zhivotovsky B. Reactive oxygen species generated in different compartments induce cell death, survival, or senescence. *Free Radic Biol Med* 57: 176–187, 2013.
159. Parsonage D, Karplus PA, and Poole LB. Substrate specificity and redox potential of AhpC, a bacterial peroxiredoxin. *Proc Natl Acad Sci U S A* 105: 8209–8214, 2008.
160. Pase L, Layton JE, Wittmann C, Ellett F, Nowell CJ, Reyes-Aldasoro CC, Varma S, Rogers KL, Hall CJ, Keightley MC, Crosier PS, Grabher C, Heath JK, Renshaw SA, and Lieschke GJ. Neutrophil-delivered myeloperoxidase dampens the hydrogen peroxide burst after tissue wounding in zebrafish. *Curr Biol* 22: 1818–1824, 2012.
161. Pase L, Nowell CJ, and Lieschke GJ. In vivo real-time visualization of leukocytes and intracellular hydrogen peroxide levels during a zebrafish acute inflammation assay. *Methods Enzymol* 506: 135–156, 2012.
162. Pearson T, Kabayo T, Ng R, Chamberlain J, McArdle A, and Jackson MJ. Skeletal muscle contractions induce acute changes in cytosolic superoxide, but slower responses in mitochondrial superoxide and cellular hydrogen peroxide. *PLoS One* 9: e96378, 2014.
163. Poburko D, Santo-Domingo J, and Demaurex N. Dynamic regulation of the mitochondrial proton gradient during cytosolic calcium elevations. *J Biol Chem* 286: 11672–11684, 2011.
164. Pollegioni L, Diederichs K, Molla G, Umhau S, Welte W, Ghisla S, and Pilone MS. Yeast D-amino acid oxidase: structural basis of its catalytic properties. *J Mol Biol* 324: 535–546, 2002.
165. Poole LB, Godzik A, Nayeem A, and Schmitt JD. AhpF can be dissected into two functional units: tandem repeats of two thioredoxin-like folds in the N-terminus mediate electron transfer from the thioredoxin reductase-like C-terminus to AhpC. *Biochemistry* 39: 6602–6615, 2000.
166. Poole LB, Karplus PA, and Claiborne A. Protein sulfenic acids in redox signaling. *Annu Rev Pharmacol Toxicol* 44: 325–347, 2004.
167. Poole LB. Bacterial defenses against oxidants: mechanistic features of cysteine-based peroxidases and their flavoprotein reductases. *Arch Biochem Biophys* 433: 240–254, 2005.
168. Porras OH and Stutzin A. Glutamate-induced metabolic changes influence the cytoplasmic redox state of hippocampal neurons. *Biochem Biophys Res Commun* 411: 82–87, 2011.
169. Poss KD, Wilson LG, and Keating MT. Heart regeneration in zebrafish. *Science* 298: 2188–2190, 2002.
170. Qi M and Elion EA. MAP kinase pathways. *J Cell Sci* 118: 3569–3572, 2005.
171. Quatresous E, Legrand C, and Pouvreau S. Mitochondria-targeted cpYFP: pH or superoxide sensor? *J Gen Physiol* 140: 567–570, 2012.
172. Rada B, Hably C, Meczner A, Timár C, Lakatos G, Enyedi P, and Ligeti E. Role of Nox2 in elimination of microorganisms. *Semin Immunopathol* 30: 237–253, 2008.
173. Raha S and Robinson BH. Mitochondria, oxygen free radicals, disease and ageing. *Trends Biochem Sci* 25: 502–508, 2000.
174. Ramming T, Hansen HG, Nagata K, Ellgaard L, and Appenzeller-Herzog C. GPx8 peroxidase prevents leakage of H_2O_2 from the endoplasmic reticulum. *Free Radic Biol Med* 70: 106–116, 2014.
175. Raya A, Koth CM, Büscher D, Kawakami Y, Itoh T, Raya RM, Sternik G, Tsai HJ, Rodríguez-Esteban C, and Izpisúa-Belmonte JC. Activation of Notch signaling pathway precedes heart regeneration in zebrafish. *Proc Natl Acad Sci U S A* 100: 11889–11895, 2003.
176. Rhee SG, Bae YS, Lee SR, and Kwon J. Hydrogen peroxide: a key messenger that modulates protein phosphorylation through cysteine oxidation. *Sci STKE* 53: 1–6, 2000.
177. Rhee SG, Chang TS, Jeong W, and Kang D. Methods for detection and measurement of hydrogen peroxide inside and outside of cells. *Mol Cells* 29: 539–549, 2010.
178. Rhee SG. Cell signaling. H_2O_2, a necessary evil for cell signaling. *Science* 312: 1882–1883, 2006.
179. Riquelme D, Alvarez A, Leal N, Adasme T, Espinoza I, Valdes JA, Troncoso N, Hartel S, Hidalgo J, Hidalgo C, and Carrasco MA. High-frequency field stimulation of primary neurons enhances ryanodine receptor-mediated Ca2+ release and generates hydrogen peroxide, which jointly stimulate NF-kappaB activity. *Antioxid Redox Signal* 14: 1245–1259, 2011.
180. Rogers C, Davis B, Neufer PD, Murphy MP, Anderson EJ, and Robidoux J. A transient increase in lipid peroxidation primes preadipocytes for delayed mitochondrial inner membrane permeabilization and ATP depletion during prolonged exposure to fatty acids. *Free Radic Biol Med* 67: 330–341, 2014.
181. Roma LP, Duprez J, Takahashi HK, Gilon P, Wiederkehr A, and Jonas JC. Dynamic measurements of mitochondrial hydrogen peroxide concentration and glutathione redox state in rat pancreatic β-cells using ratiometric fluorescent proteins: confounding effects of pH with HyPer but not roGFP1. *Biochem J* 441: 971–978, 2012.
182. Ronen M, Shalaby S, and Horwitz BA. Role of the transcription factor ChAP1 in cytoplasmic redox homeostasis: imaging with a genetically encoded sensor in the maize pathogen *Cochliobolus heterostrophus*. *Mol Plant Pathol* 14: 786–790, 2013.

183. Rota C, Chignell CF, and Mason RP. Evidence for free radical formation during the oxidation of 2′-7′-dichlorofluorescin to the fluorescent dye 2′-7′-dichlorofluorescein by horseradish peroxidase: possible implications for oxidative stress measurements. *Free Radic Biol Med* 27: 873–881, 1999.
184. Rota C, Fann YC, and Mason RP. Phenoxyl free radical formation during the oxidation of the fluorescent dye 2′,7′-dichlorofluorescein by horseradish peroxidase. Possible consequences for oxidative stress measurements. *J Biol Chem* 274: 28161–28168, 1999.
185. Saadeh M, Ferrante TC, Kane A, Shirihai O, Corkey BE, and Deeney JT. Reactive oxygen species stimulate insulin secretion in rat pancreatic islets: studies using monooleoyl-glycerol. *PLoS One* 7: e30200, 2012.
186. Sartoretto JL, Kalwa H, Pluth MD, Lippard SJ, and Michel T. Hydrogen peroxide differentially modulates cardiac myocyte nitric oxide synthesis. *Proc Natl Acad Sci U S A* 108: 15792–15797, 2011.
187. Schmitt FJ, Thaa B, Junghans C, Vitali M, Veit M, and Friedrich T. eGFP-pHsens as a highly sensitive fluorophore for cellular pH determination by fluorescence lifetime imaging microscopy (FLIM). *Biochim Biophys Acta* 1837: 1581–1593, 2014.
188. Schwarzländer M, Dick TP, Meye AJ, and Morgan B. Dissecting redox biology using fluorescent protein sensors. *Antioxid Redox Signal* 24: 680–712.
189. Schwarzländer M, Logan DC, Fricker MD, and Sweetlove LJ. The circularly permuted yellow fluorescent protein cpYFP that has been used as a superoxide probe is highly responsive to pH but not superoxide in mitochondria: implications for the existence of superoxide 'flashes'. *Biochem J* 437: 381–387, 2011.
190. Sen CK and Roy S. Redox signals in wound healing. *Biochim Biophys Acta* 1780: 1348–1361, 2008.
191. Sevier CS, Qu H, Heldman N, Gross E, Fass D, and Kaiser CA. Modulation of cellular disulfide-bond formation and the ER redox environment by feedback regulation of Ero1. *Cell* 129: 333–344, 2007.
192. Shi Y, Zhang Y, Zhao F, Ruan H, Huang H, Luo L, and Li L. Acetylcholine serves as a derepressor in loperamide-induced opioid-induced bowel dysfunction (OIBD) in zebrafish. *Sci Rep* 4: 5602, 2014.
193. Sies H. Role of metabolic H_2O_2 generation: redox signaling and oxidative stress. *J Biol Chem* 13: 8735–8741, 2014.
194. Son JK, Varadarajan S, and Bratton SB. TRAIL-activated stress kinases suppress apoptosis through transcriptional upregulation of MCL-1. *Cell Death Differ* 17: 1288–1301, 2010.
195. Soto MA, González C, Lissi E, Vergara C, and Latorre R. Ca(2+)-activated K+ channel inhibition by reactive oxygen species. *Am J Physiol Cell Physiol* 282: C461–C471, 2002.
196. Starkov AA, Polster BM, and Fiskum G. Regulation of hydrogen peroxide production by brain mitochondria by calcium and Bax. *J Neurochem* 83: 220–228, 2002.
197. Stone JR and Yang S. Hydrogen peroxide: a signaling messenger. *Antioxid Redox Signal* 8: 243–270, 2006.
198. Storz G and Imlay JA. Oxidative stress. *Curr Opin Microbiol* 2: 188–194, 1999.
199. Stoyanovsky DA, Huang Z, Jiang J, Belikova NA, Tyurin V, Epperly MW, Greenberger JS, Bayir H, and Kagan VE. A manganese-porphyrin complex decomposes H(2)O(2), inhibits apoptosis, and acts as a radiation mitigator in vivo. *ACS Med Chem Lett* 2: 814–817, 2011.
200. St-Pierre J, Buckingham JA, Roebuck SJ, and Brand MD. Topology of superoxide production from different sites in the mitochondrial electron transport chain. *J Biol Chem* 277: 44784–44790, 2002.
201. Sun Q, Gao W, Loughran P, Shapiro R, Fan J, Billiar TR, and Scott MJ. Caspase 1 activation is protective against hepatocyte cell death by up-regulating beclin 1 protein and mitochondrial autophagy in the setting of redox stress. *J Biol Chem* 288: 15947–15958, 2013.
202. Suzuki N, Koussevitzky S, Mittler R, and Miller G. ROS and redox signalling in the response of plants to abiotic stress. *Plant Cell Environ* 35: 259–270, 2012.
203. Tang XD, Santarelli LC, Heinemann SH, and Hoshi T. Metabolic regulation of potassium channels. *Annu Rev Physiol* 66: 131–159, 2004.
204. Tavender TJ and Bulleid NJ. Peroxiredoxin IV protects cells from oxidative stress by removing H_2O_2 produced during disulphide formation. *J Cell Sci* 123: 2672–2679, 2010.
205. Tavender TJ, Sheppard AM, and Bulleid NJ. Peroxiredoxin IV is an endoplasmic reticulum-localized enzyme forming oligomeric complexes in human cells. *Biochem J* 411: 191–199, 2008.
206. Treiber N, Maity P, Singh K, Kohn M, Keist AF, Ferchiu F, Sante L, Frese S, Bloch W, Kreppel F, Kochanek S, Sindrilaru A, Iben S, Högel J, Ohnmacht M, Claes LE, Ignatius A, Chung JH, Lee MJ, Kamenisch Y, Berneburg M, Nikolaus T, Braunstein K, Sperfeld AD, Ludolph AC, Briviba K, Wlaschek M, Florin L, Angel P, and Scharffetter-Kochanek K. Accelerated aging phenotype in mice with conditional deficiency for mitochondrial superoxide dismutase in the connective tissue. *Aging Cell* 10: 239–254, 2011.
207. Treiber N, Peters T, Sindrilaru A, Huber R, Kohn M, Menke A, Briviba K, Kreppel F, Basu A, Maity P, Koller M, Iben S, Wlaschek M, Kochanek S, and Scharffetter-Kochanek K. Overexpression of manganese superoxide dismutase in human dermal fibroblasts enhances the contraction of free floating collagen lattice: implications for ageing and hyperplastic scar formation. *Arch Dermatol Res* 301: 273–287, 2009.
208. Ungvari Z, Labinskyy N, Mukhopadhyay P, Pinto JT, Bagi Z, Ballabh P, Zhang C, Pacher P, and Csiszar A. Resveratrol attenuates mitochondrial oxidative stress in coronary arterial endothelial cells. *Am J Physiol Heart Circ Physiol* 297: H1876–H1881, 2009.
209. Varnai P and Balla T. Live cell imaging of phosphoinositide dynamics with fluorescent protein domains. *Biochim Biophys Acta* 1761: 957–967, 2006.
210. Veal EA, Day AM, and Morgan BA. Hydrogen peroxide sensing and signaling. *Mol Cell* 26: 1–14, 2007.
211. Wallace DC. Mitochondrial diseases in man and mouse. *Science* 283: 1482–1488, 1999.
212. Wang H, Karadge U, Humphries WH 4th, and Fisher AL. Analyzing cell physiology in *Caenorhabditis elegans* with fluorescent ratiometric reporters. *Methods* 68: 508–517, 2014.
213. Weissmann N, Sydykov A, Kalwa H, Storch U, Fuchs B, Mederos y Schnitzler M, Brandes RP, Grimminger F, Meissner M, Freichel M, Offermanns S, Veit F, Pak O, Krause KH, Schermuly RT, Brewer AC, Schmidt HH, Seeger W, Shah AM, Gudermann T, Ghofrani HA, and Dietrich A. Activation of TRPC6 channels is essential for lung ischaemia-reperfusion induced oedema in mice. *Nat Commun* 3: 649, 2012.
214. Weller J, Kizina KM, Can K, Bao G, and Müller M. Response properties of the genetically encoded optical H_2O_2 sensor HyPer. *Free Radic Biol Med* 76: 227–241, 2014.

215. Weyemi U, Lagente-Chevallier O, Boufraqech M, Prenois F, Courtin F, Caillou B, Talbot M, Dardalhon M, Al Ghuzlan A, Bidart JM, Schlumberger M, and Dupuy C. ROS-generating NADPH oxidase NOX4 is a critical mediator in oncogenic H-Ras-induced DNA damage and subsequent senescence. *Oncogene* 31: 1117–1129, 2012.
216. Wiemer M and Osiewacz HD. Effect of paraquat-induced oxidative stress on gene expression and aging of the filamentous ascomycete *Podospora anserina*. *Microbial Cell* 1: 225–240, 2014.
217. Winterbourn CC and Hampton MB. Thiol chemistry and specificity in redox signaling. *Free Radic Biol Med* 45: 549–561, 2008.
218. Wood ZA, Poole LB, and Karplus PA. Peroxiredoxin evolution and the regulation of hydrogen peroxide signaling. *Science* 300: 650–653, 2003.
219. Wood ZA, Schröder E, Robin Harris J, and Poole LB. Structure, mechanism and regulation of peroxiredoxins. *Trends Biochem Sci* 28: 32–40, 2003.
220. Wu RF, Ma Z, Liu Z, and Terada LS. Nox4-derived H_2O_2 mediates endoplasmic reticulum signaling through local Ras activation. *Mol Cell Biol* 30: 3553–3568, 2010.
221. Yan B, Han P, Pan L, Lu W, Xiong J, Zhang M, Zhang W, Li L, and Wen Z. IL-1β and reactive oxygen species differentially regulate neutrophil directional migration and Basal random motility in a zebrafish injury-induced inflammation model. *J Immunol* 192: 5998–6008, 2014.
222. Ye F, Zhou F, Bedolla RG, Jones T, Lei X, Kang T, Guadalupe M, and Gao SJ. Reactive oxygen species hydrogen peroxide mediates Kaposi's sarcoma-associated herpesvirus reactivation from latency. *PLoS Pathog* 7: e1002054, 2011.
223. Yoo SK, Starnes TW, Deng Q, and Huttenlocher A. Lyn is a redox sensor that mediates leukocyte wound attraction in vivo. *Nature* 480: 109–112, 2011.
224. Yu Q, Lee CF, Wang W, Karamanlidis G, Kuroda J, Matsushima S, Sadoshima J, and Tian R. Elimination of NADPH oxidase activity promotes reductive stress and sensitizes the heart to ischemic injury. *J Am Heart Assoc* 3: e000555, 2014.
225. Zhao Y, Araki S, Wu J, Teramoto T, Chang YF, Nakano M, Abdelfattah AS, Fujiwara M, Ishihara T, Nagai T, and Campbell RE. An expanded palette of genetically encoded Ca(2+) indicators. *Science* 333: 1888–1891, 2011.
226. Zhao Y, Jin J, Hu Q, Zhou HM, Yi J, Yu Z, Xu L, Wang X, Yang Y, and Loscalzo J. Genetically encoded fluorescent sensors for intracellular NADH detection. *Cell Metab* 14: 555–566, 2011.
227. Zheng M, Aslund F, and Storz G. Activation of the OxyR transcription factor by reversible disulfide bond formation. *Science* 279: 1718–1721, 1998.

Address correspondence to:
Dr. Vsevolod V. Belousov
Shemyakin-Ovchinnikov Institute of Bioorganic Chemistry
Moscow 117997
Russia

E-mail: vsevolod.belousov@gmail.com

Date of first submission to ARS Central, November 23, 2015; date of acceptance, November 25, 2015.

Abbreviations Used

Anti-CD3/CD28 = antibodies against cluster of differentiation (CD) 3/28
Apo2L/TRAIL = Apo2 ligand or tumor necrosis factor (TNF)-related apoptosis-inducing ligand
BTK = Bruton's tyrosine kinase
cpYFP = circularly permuted yellow fluorescent protein
DAO = D-amino acid oxidase
DCFH = 2,7-dichlorodihydrofluorescein
DHR = dihydrorhodamine 123
DTT = dithiothreitol
Duox = dual oxidase
EGF = epidermal growth factor
EGFP = enhanced green fluorescent protein
EGFR = epidermal growth factor receptor
ER = endoplasmic reticulum
ERK = extracellular signal-regulated kinases
FLIM = fluorescence lifetime imaging microscopy
FPs = fluorescent proteins
GFP = green fluorescent protein
GPx = glutathione peroxidases
Grx = glutaredoxin
GSH = glutathione (reduced state)
GSSG = glutathione disulfide (oxidized glutathione)
H_2O_2 = hydrogen peroxide
JNK = jun N-terminal kinase
MAPKs = mitogen-activated protein kinases
NGF = nerve growth factor
NOSs = nitric oxide synthases
PC1 = Peroxy Crimson 1
PDGF = platelet-derived growth factor
PG1 = Peroxy Green 1
PI = phosphatidylinositol
PI3K = phosphatidylinositol 3-kinase
PIP3 = phosphatidylinositol 3,4,5-trisphosphate
PIP-SHOW = PIP3 and SH Oxidation Watching
Prxs = peroxiredoxins
PTKs = protein tyrosine kinases
PTPs = protein tyrosine phosphatases
roGFPs = redox green fluorescent proteins
ROS = reactive oxygen species
rxYFP = redox yellow fluorescent protein
RyR = ryanodine receptor
SOD = superoxide dismutase
TG = thapsigargin
T_H = T helper
TMRM = tetramethylrhodamine methyl ester
TNF-α = tumor necrosis factor alpha
Trxs = thioredoxins